

Final Report on the Torque Key Comparison CCM.T-K1 Measurand Torque: 0 N·m, 500 N·m, 1000 N·m

Pilot Laboratory: Physikalisch-Technische Bundesanstalt (PTB)
Contact Person: Dr. Dirk Röske
Address: Physikalisch-Technische Bundesanstalt
Department 1.2 “Solid Mechanics”
Working Group 1.22 “Torque Realization”
Bundesallee 100
D-38116 Braunschweig
Germany
Phone: +49 531-592 1131
Fax: +49 531-592 691131
E-Mail: dirk.roeske@ptb.de

This report includes the following sections:

1. **General information about the CCM.T-K1**
 2. **Principles of the comparison**
 3. **Realisation of the comparison**
 4. **Limitations of the comparison**
 5. **Uniformity of the measured values**
 6. **Characteristics of the transducers**
 7. **Results of the measurements: reported deflections and uncertainties, calculated corrections**
 8. **Summary**
- Annexes**
- A.1 **Weighted means, χ^2 tests and key comparison reference values**
 - A.2 **Relative deviations of the results from the reference values**
 - A.3 **Degrees of equivalence**

1. General information about the CCM.T-K1

In March 2004 in Pretoria (South Africa) the CCM force working group, chaired at that time by Prof. Manfred Peters (PTB), decided to carry out CIPM torque key comparisons. Two ranges were agreed – 1 kN·m and 20 kN·m. As pilot laboratory for both inter-comparisons the torque working group of PTB was appointed [1]. This is the report for the 1 kN·m key comparison denoted as CCM.T-K1. Eight laboratories - including the pilot - took part in the key comparison (see table 1).

Table1: Participants in the CCM.T-K1 torque key comparisons: countries, institutes and code numbers used in the report

Country (alphabetical order)	Institute	Code letter
Brazil	INMETRO	E
Germany	PTB	H
Japan	NMIJ	D
Korea	KRISS	C
Mexico	CENAM	F
Spain	CEM	B
Switzerland	METAS	A
United Kingdom	NPL	G

2. Principles of the comparison

The purpose of key comparisons is to compare the units of the given quantities as realized throughout the world. In the field of torque, this is done by using torque transducers of high quality, high-precision frequency-carrier amplifiers and very stable bridge standards. The torque transducers were subject to similar loading schemes in the torque standard machines of the participants following a strict measurement protocol and using similar amplifiers. The following loading scheme was agreed:

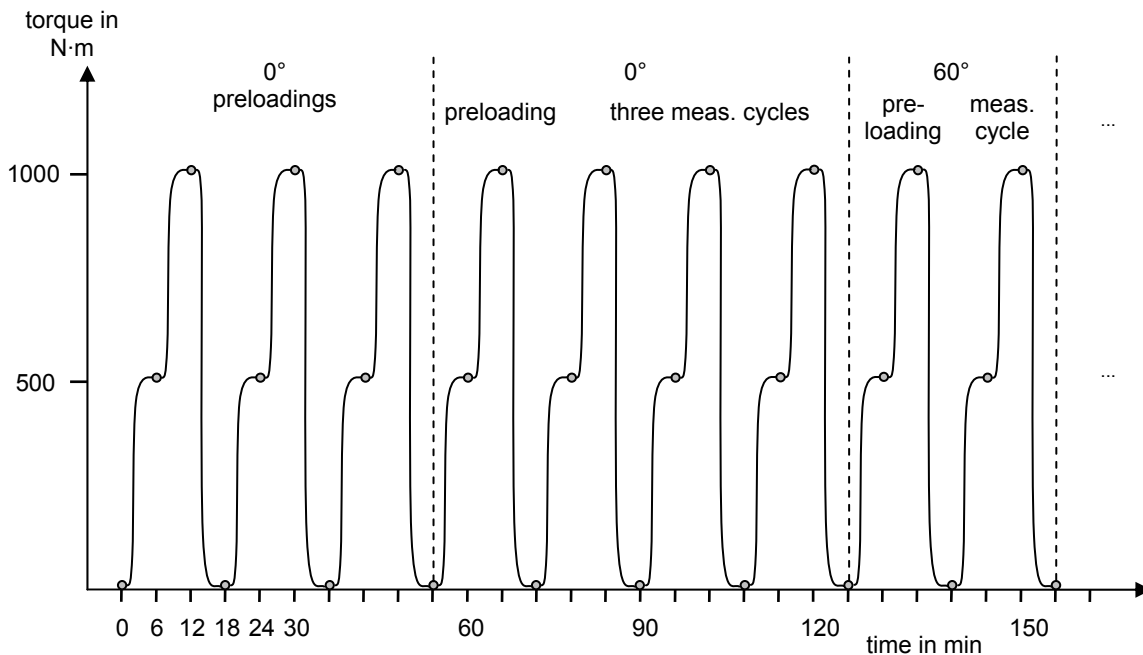


Figure 1. Diagram of the measurement sequence of the CCM.T-K1

The torque transducer was rotated from 0° to 720° with 60° steps. Except the first mounting position with seven load cycles – four for stabilization and three for the repeatability measurement - in all other positions one preload and one measurement cycle (as shown for the 60° position in figure 1) were carried out, i.e. at transducer positions of 120°, 180°, 240°, 300°, 360°, 420°, 480°, 540°, 600°, 660° and 720°.

The comparison measurements had to be done with each of two torque transducers having nominal capacities of 1 kN·m. The first transducer is a TB2 torque measuring flange with adaptors at both ends. The second transducer is a TT1 transducer of shaft type. The construction principles of the two transducer types are different, but the mechanical interface is the same – round shafts with 50 mm diameter and a suitable length fitting for an ETP-50 hydraulic coupling. The transducers had been selected for their very stable characteristics and their known history.

3. Realisation of the comparison

For this key comparison a star type formation had been chosen. That means that the transducers were returned to the pilot laboratory after the measurement at each participant. The pilot repeated all measurements before sending the instruments to the next participant. One complete measurement cycle (pilot – participating laboratory – pilot) is called a loop. The first measurement by the pilot is called the “H1” measurement and the second measurement by the pilot after the participating laboratory is called the “H2” measurement. In general, a “H2” measurement for one participant is the “H1” measurement for the next participant, if there is one.

4. Limitations of the comparison

In 6 it will be shown, that the travelling standards (transducers TB2 and TT1) used in this key comparison were very stable, especially the hermetically closed TB2 [2]. Nevertheless, in order to get comparable results some known effects should be taken into account. These are possible deviations of the amplifiers (DMP40) of the participating laboratories, the creep influence due to different loading times in the machines and the environmental conditions on site.

Due to the fact that there is no real reference value (the transfer transducers do not provide constant values), the following facts should be accepted: there is no absolute numerical reference value and only relative deviations can be compared.

5. Uniformity of the measured values

In practice, it is not possible to calibrate the DMP40 amplifiers of the participating laboratories against an absolute reference standard. The uniformity of the different DMP40s was confirmed with reference to a BN100 bridge standard. Each participating laboratory measured the indication of its own DMP40 against the signal of the pilot's BN100, which was delivered together with the transducers. The pilot monitored the signal of the same BN100 against two DMP40 amplifiers in the pilot laboratory additionally each time when the equipment was back from a participant. The sensitivities of the transducers at nominal torque were 1.000 mV/V (TB2) and 1.342 mV/V (TT1). The measurements with the BN100 were carried out with suitably selected voltage ratios near the signals of the transducers for 500 N·m and 1 kN·m. Therefore, figure 2 shows two lines for positive and two lines for negative voltage ratios for each of the participants.

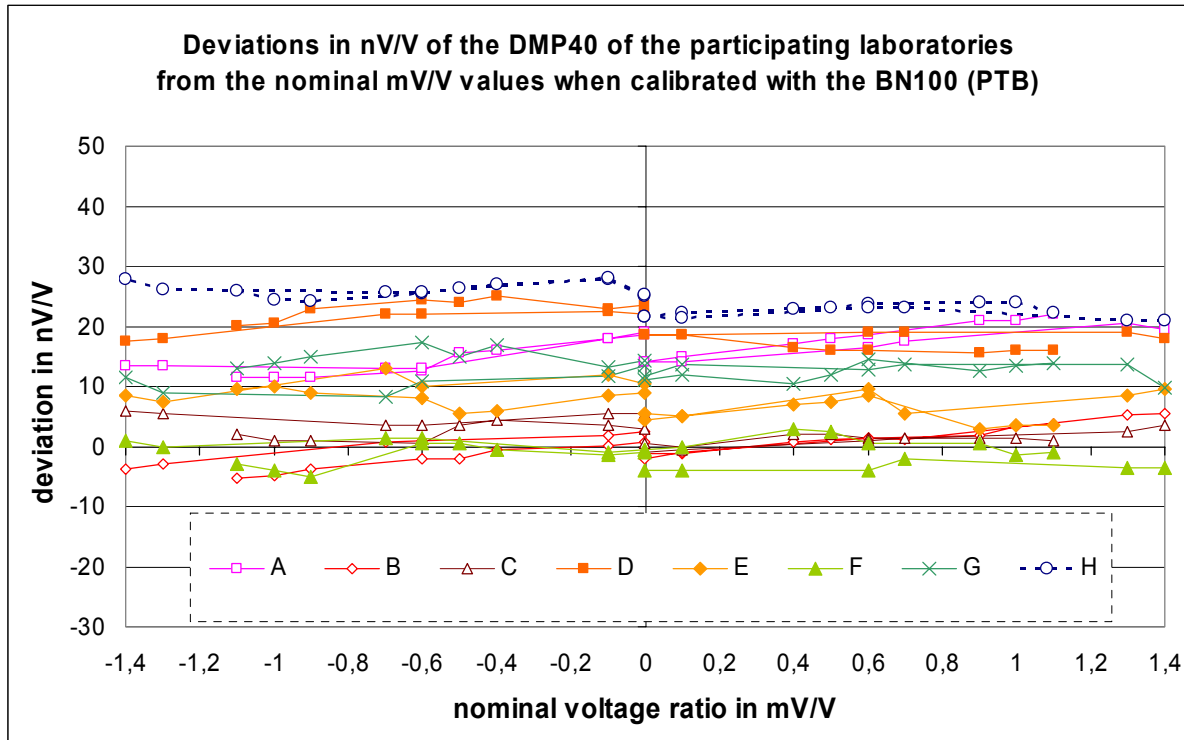


Figure 2. Deviations in nV/V of the DMP40 indication of the participating laboratories from the nominal mV/V values when calibrated with the pilot's BN100 (averaged values from two measurements, for the pilot H averaged over 16 measurements)

These measurements show that there are quite large deviations of up to 32 nV/V between the different DMPs. But the measurement result is a difference between two readings, that means an offset of the DMP's indication as shown in figure 2 will not affect the results as long as these functions have no slope. The relative deviations of the voltage ratio differences (referred to the signal at nominal zero given by the BN100) from their nominal value are shown for all DMPs in table 2.

Table 2: Relative deviations d_i of the zero-related voltage ratio differences of the participants' DMPs from their nominal values

	nominal voltage ratio difference in mV/V	relative voltage ratio difference* d_i related to nominal value for lab ...							
		... A in ppm	... B in ppm	... C in ppm	... D in ppm	... E in ppm	... F in ppm	... G in ppm	... H in ppm
TB2 cw**	0.5	8.0	4.7	3.0	-5.0	6.0	6.0	1.5	3.1
	1	3.0	2.2	-0.5	-2.5	-4.0	-4.0	1.5	0.8
TB2 acw**	-0.5	7.0	5.7	-1.0	-1.0	7.0	-3.0	-1.3	-2.9
	-1	4.0	2.9	2.5	3.0	-4.5	4.5	1.2	2.0
TT1 cw	0.67***	4.8	4.8	3.5	0.7	1.8	2.1	2.4	2.3
	1.34***	2.2	3.1	1.2	0.1	1.6	-0.7	-1.0	-1.7
TT1 acw	-0.67***	8.2	2.2	3.0	0.0	-2.4	-3.0	6.4	-0.8
	-1.34***	-0.4	3.1	-1.6	3.1	3.1	0.8	-0.6	-0.9

* related to nominal 0 mV/V, ** cw – clockwise, acw – anti-clockwise, *** interpolated

Using the values $d_i(V/V_S)$ given in table 2 for each of the participants and the corresponding voltage ratios V/V_S , the deflections calculated from the participant's calibration results can be corrected using (1):

$$Y_i' = Y_i \cdot (1 - d_i(V/V_S)) \quad (1)$$

with Y_i being the uncorrected and Y_i' the corrected deflections.

6. Characteristics of the transducers

Creep effect

To minimize the influence of the creep, a relatively long cycle time of 6 minutes was agreed. This time includes the loading/unloading and the waiting time before the reading. The creep effect should be small enough to eliminate the uncertainty of the time of reading for every loading.

Both transducers had a nearly constant creep after approx. 3 min, i.e. the values showed a quite linear dependence on the time. The relative change of the indication due to creep for a period from the 4th, resp. the 5th, to the 6th minute after the torque application is given in table 3 for both transducers at 1 kN·m torque. The values indicate that a change in the reading time by some seconds is not significant to the uncertainty of measurement.

Table 3: Relative change of indication due to creep at 1 kN·m

	Relative change of indication due to creep	
Time after start of load application	TB2, S/N #044430025/1 kN·m	TT1, S/N 36079-00
4 th to 6 th minute after applying the load	$4 \cdot 10^{-6}$	$4 \cdot 10^{-6}$
5 th to 6 th minute after applying the load	$2 \cdot 10^{-6}$	$2 \cdot 10^{-6}$

The aim was to have an equal loading schedule for each laboratory, but this could not be realized due to the different designs and capabilities of the machines. The loading times varied from 25 s to 150 s. The shortest time for taking the readings after finishing the torque application was 3.5 min. The pilot checked the loading time with the transducer TB2, S/N #044430025/1 kN·m. The difference between loading times of 23 s and 42 s in the PTB's 1 kN·m torque standard machine gave a difference after the 6 min of only $1 \cdot 10^{-6}$, which is less than any measurement uncertainty. Table 4 shows the time needed for the torque application (from 0 N·m to 500 N·m, respectively from 500 N·m to 1 kN·m) in the different standard machines of the participants. A long torque application time and a fast loading speed mean, that the load is applied in a short time after a longer waiting time (for collecting the weights, for example). A slow loading speed means, that the quite long torque application time is needed to apply the weights one by one.

Depending on the loading profile (time and speed) of the machines, different correction factors are proposed and should be used in order to reduce the creep influence on the result.

Table 4: Time needed for the application of the torque and correction factors

Participant	Torque application time		Time difference to pilot		Loading speed	Correction factor c_i for	
	in s	in min	in s	in min		500 N·m	1000 N·m
A	60	1.0	35	0.58	fast	1	1
B	30	0.5	5	0.08	fast	1	1
C	60	1.0	35	0.58	fast	1	1
D	130	2.17	105	1.75	slow	$(1 + 4 \cdot 10^{-6})$	$(1 + 2 \cdot 10^{-6})$
E	150	2.5	125	2.08	fast	$(1 + 6 \cdot 10^{-6})$	$(1 + 3 \cdot 10^{-6})$
F	90	1.5	65	1.08	slow	$(1 + 2 \cdot 10^{-6})$	$(1 + 1 \cdot 10^{-6})$
G	100	1.67	75	1.25	slow	$(1 + 2 \cdot 10^{-6})$	$(1 + 1 \cdot 10^{-6})$
H	25	0.42	-	-	fast	1	1

Using the values c_i given in table 4 for each of the participants, the deflections calculated from the participant's calibration results can be corrected using (2):

$$Y_i'' = Y_i' \cdot c_i \quad (2)$$

with Y_i' being the uncorrected and Y_i'' the corrected deflections.

Humidity and temperature influences on the sensitivity

The humidity effect on the sensitivity can be an important factor if the environmental humidity at the participating laboratory is not the same as that at the pilot. For determining the humidity sensitivity e_{RH} of

each transducer, measurements at a 5%rH higher humidity level have been carried out in clockwise direction.

The temperature effect on the sensitivity can also be an important factor if the environmental temperature in the participating laboratory is not the same as that at the pilot. For determining the temperature sensitivity e_T of each transducer, measurements at a 5°C higher temperature level have been carried out in clockwise direction.

The result reported in [1] could be confirmed. Due to its closed design the TB2 transducer was nearly insensitive to changes of the relative humidity, whereas the TT1 transducer showed a quite strong dependence on the humidity of the ambient air (see Fig. 3 to 6). And the TB2 transducer was also less sensitive to changes of the temperature compared with the TT1 transducer (see figures 7 to 10).

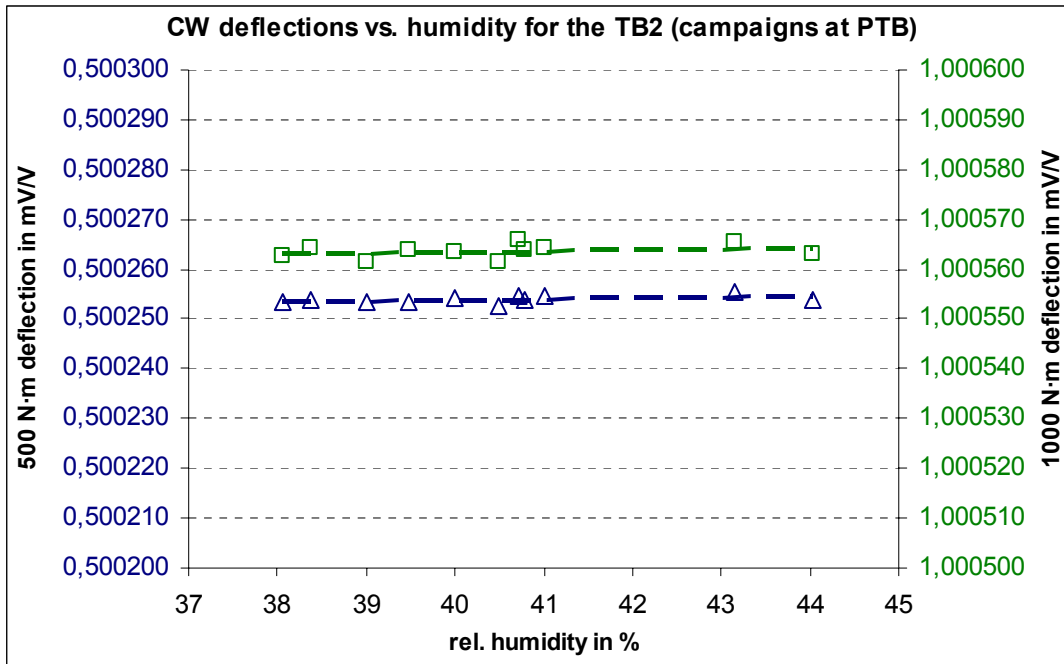


Figure 3. Clockwise deflections in mV/V of the TB2 measured during campaigns at the pilot laboratory vs. relative air humidity: for 500 N-m (triangles, left axis of ordinates) and 1000 N-m (squares, right axis of ordinates), scaling range: 100 nV/V, temperature influence corrected

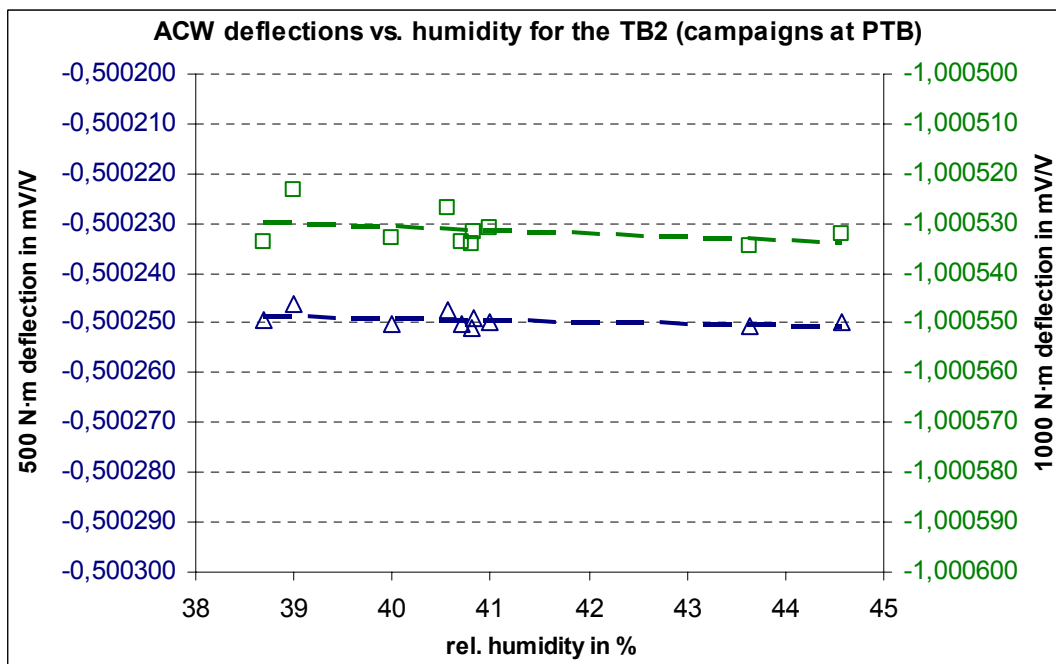


Figure 4. Anti-clockwise deflections in mV/V of the TB2 measured during campaigns at the pilot laboratory vs. relative air humidity: for 500 N-m (triangles, left axis of ordinates) and 1000 N-m (squares, right axis of ordinates), scaling range: 100 nV/V, temperature influence corrected

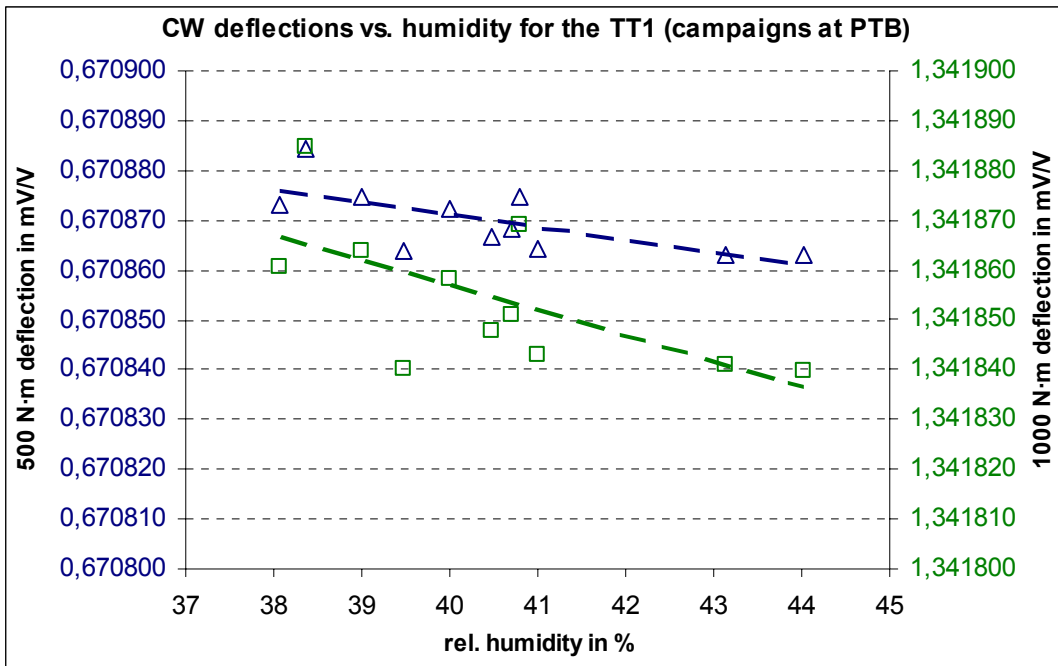


Figure 5. Clockwise deflections in mV/V of the TT1 measured during campaigns at the pilot laboratory vs. relative air humidity: for 500 N·m (triangles, left axis of ordinates) and 1000 N·m (squares, right axis of ordinates), scaling range: 100 nV/V, temperature influence corrected

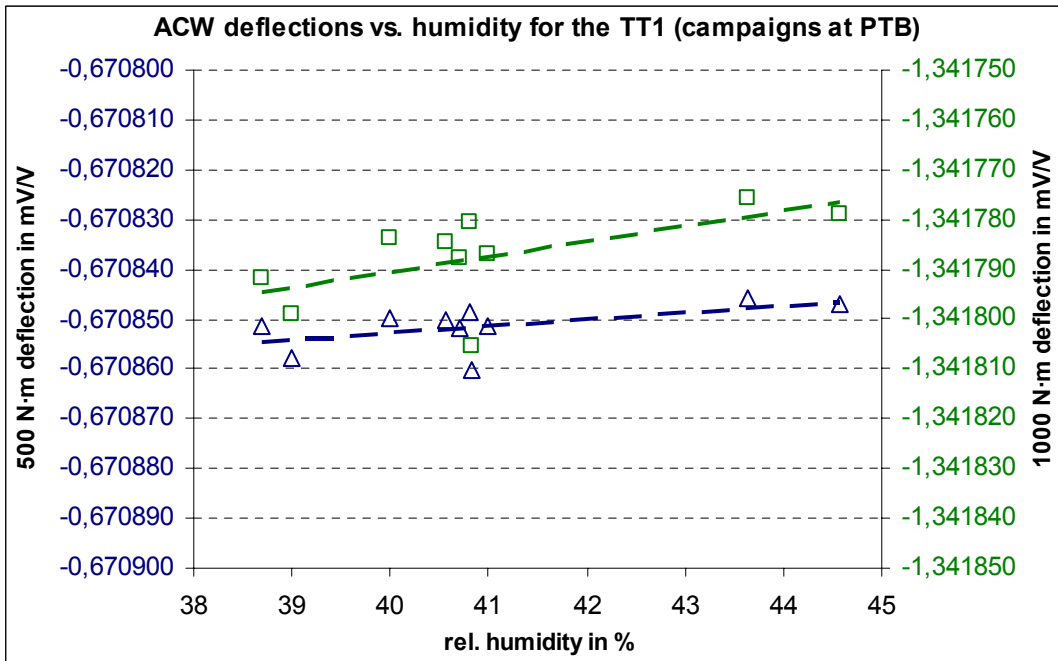


Figure 6. Anti-clockwise deflections in mV/V of the TT1 measured during campaigns at the pilot laboratory vs. relative air humidity: for 500 N·m (triangles, left axis of ordinates) and 1000 N·m (squares, right axis of ordinates), scaling range: 100 nV/V, temperature influence corrected

It is considered that the humidity and temperature sensitivities have the same absolute value for clockwise and anti-clockwise torque, therefore only clockwise measurements have been carried out. All measurements at the pilot as participant together with the additional measurements at higher temperature, respectively humidity were used to calculate the corresponding sensitivities of the transducers for both torque steps. For this purpose, a linear regression according to (3) was used.

$$S_i = S_0 + e_{rH} \cdot \Delta rH_i + e_T \cdot \Delta T_i \quad (3)$$

with S_0 being the deflection at reference conditions and S_i the deflection at conditions changed by ΔrH_i and ΔT_i .

The values obtained in this calculation are given in table 5. The corresponding uncertainties take into account the uncertainty propagation in (3) as well as the contribution of the fitting procedure (scattering of the data) according to

$$u^2(e_{rH}) = u^2(e_{rH})_{\text{prop}} + u^2(e_{rH})_{\text{fit}} \quad \text{and} \quad u^2(e_T) = u^2(e_T)_{\text{prop}} + u^2(e_T)_{\text{fit}} \quad (4)$$

with $u^2(e_{rH})_{\text{fit}}$ and $u^2(e_T)_{\text{fit}}$ calculated as standard deviation of the estimator using Excel's RGP function.

The first contribution in (4) and (5) was estimated using two data sets, the one with the higher relative humidity and the one with the higher temperature. In this case, equation (3) writes as

$$\begin{aligned} S_1 &= S_0 + e_{rH} \cdot \Delta rH_1 + e_T \cdot \Delta T_1 \\ S_2 &= S_0 + e_{rH} \cdot \Delta rH_2 + e_T \cdot \Delta T_2 \end{aligned} \quad (5)$$

and e_{rH} and e_T can be found from (6)

$$e_{rH} = \frac{(S_1 - S_0) \cdot \Delta T_2 - (S_2 - S_0) \cdot \Delta T_1}{\Delta rH_1 \cdot \Delta T_2 - \Delta rH_2 \cdot \Delta T_1} \quad \text{and} \quad e_T = \frac{(S_1 - S_0) \cdot \Delta rH_2 - (S_2 - S_0) \cdot \Delta rH_1}{\Delta T_1 \cdot \Delta rH_2 - \Delta T_2 \cdot \Delta rH_1} \quad (6)$$

With $S_i - S_0 = \Delta S_i$, $u^2(\Delta S_i) = u^2(\Delta S)$, $u^2(\Delta rH_i) = u^2(\Delta rH)$ and $u^2(\Delta T_i) = u^2(\Delta T)$ for $i \in \{1, 2\}$ the combined variances $u^2(e_{rH})_{\text{prop}}$ and $u^2(e_T)_{\text{prop}}$ can be calculated according to (7)

$$\begin{aligned} u^2(e_{rH}) &= \left(\frac{\Delta T_2 - \Delta T_1}{\Delta rH_1 \cdot \Delta T_2 - \Delta rH_2 \cdot \Delta T_1} \right)^2 u^2(\Delta S) + \left[\frac{(\Delta T_1 - \Delta T_2)(\Delta S_1 \cdot \Delta T_2 - \Delta S_2 \cdot \Delta T_1)}{(\Delta rH_1 \cdot \Delta T_2 - \Delta rH_2 \cdot \Delta T_1)^2} \right]^2 u^2(\Delta rH) + \\ &+ \left(\frac{\Delta S_1 - \Delta S_2}{\Delta rH_1 \cdot \Delta T_2 - \Delta rH_2 \cdot \Delta T_1} \right)^2 u^2(\Delta T) + \left[\frac{(\Delta rH_2 - \Delta rH_1)(\Delta S_1 \cdot \Delta T_2 - \Delta S_2 \cdot \Delta T_1)}{(\Delta rH_1 \cdot \Delta T_2 - \Delta rH_2 \cdot \Delta T_1)^2} \right]^2 u^2(\Delta T) \\ u^2(e_T) &= \left(\frac{\Delta rH_2 - \Delta rH_1}{\Delta T_1 \cdot \Delta rH_2 - \Delta T_2 \cdot \Delta rH_1} \right)^2 u^2(\Delta S) + \left[\frac{(\Delta rH_1 - \Delta rH_2)(\Delta S_1 \cdot \Delta rH_2 - \Delta S_2 \cdot \Delta rH_1)}{(\Delta T_1 \cdot \Delta rH_2 - \Delta T_2 \cdot \Delta rH_1)^2} \right]^2 u^2(\Delta T) + \\ &+ \left(\frac{\Delta S_1 - \Delta S_2}{\Delta T_1 \cdot \Delta rH_2 - \Delta T_2 \cdot \Delta rH_1} \right)^2 u^2(\Delta rH) + \left[\frac{(\Delta T_2 - \Delta T_1)(\Delta S_1 \cdot \Delta rH_2 - \Delta S_2 \cdot \Delta rH_1)}{(\Delta T_1 \cdot \Delta rH_2 - \Delta T_2 \cdot \Delta rH_1)^2} \right]^2 u^2(\Delta rH). \end{aligned} \quad (7)$$

The following values have been used

$$\begin{aligned} \text{TB2:} \quad \Delta T_1 &= 0 \text{ K}, & \Delta rH_1 &= 5\%, & \Delta S_1 &= 1 \text{ nV/V (500 N}\cdot\text{m)}, & \Delta S_1 &= 3 \text{ nV/V (1000 N}\cdot\text{m)} \\ & \Delta T_2 &= 5.2 \text{ K}, & \Delta rH_2 &= -1\%, & \Delta S_1 &= 3 \text{ nV/V (500 N}\cdot\text{m)}, & \Delta S_1 &= 6 \text{ nV/V (1000 N}\cdot\text{m)} \\ \text{TT1:} \quad \Delta T_1 &= 0 \text{ K}, & \Delta rH_1 &= 5\%, & \Delta S_1 &= -8 \text{ nV/V (500 N}\cdot\text{m)}, & \Delta S_1 &= -24 \text{ nV/V (1000 N}\cdot\text{m)} \\ & \Delta T_2 &= 5.2 \text{ K}, & \Delta rH_2 &= -1\%, & \Delta S_1 &= 0 \text{ nV/V (500 N}\cdot\text{m)}, & \Delta S_1 &= 4 \text{ nV/V (1000 N}\cdot\text{m)} \end{aligned} \quad (8)$$

$u(\Delta S) = 1 \text{ nV/V}$ $u(\Delta rH) = 1\%$ $u(\Delta T) = 0,1 \text{ K}$

yielding standard uncertainty contributions of

$$\begin{aligned} \text{TB2:} \quad u(e_{rH})_{\text{prop}} &= 0.20 \text{ (nV/V)/\% (500 N}\cdot\text{m)} & u(e_{rH})_{\text{prop}} &= 0.20 \text{ (nV/V)/\% (1000 N}\cdot\text{m)} \\ u(e_T)_{\text{prop}} &= 0.27 \text{ (nV/V)/K (500 N}\cdot\text{m)} & u(e_T)_{\text{prop}} &= 0.36 \text{ (nV/V)/K (1000 N}\cdot\text{m)} \\ \text{TT1:} \quad u(e_{rH})_{\text{prop}} &= 0.56 \text{ (nV/V)/\% (500 N}\cdot\text{m)} & u(e_{rH})_{\text{prop}} &= 1.16 \text{ (nV/V)/\% (1000 N}\cdot\text{m)} \\ u(e_T)_{\text{prop}} &= 0.46 \text{ (nV/V)/K (500 N}\cdot\text{m)} & u(e_T)_{\text{prop}} &= 1.08 \text{ (nV/V)/K (1000 N}\cdot\text{m)}. \end{aligned} \quad (9)$$

Together with the standard uncertainty contributions $u^2(e_{rH})_{\text{fit}}$ and $u^2(e_T)_{\text{fit}}$

$$\begin{aligned} \text{TB2:} \quad u(e_{rH})_{\text{fit}} &= 0.14 \text{ (nV/V)/\% (500 N}\cdot\text{m)} & u(e_{rH})_{\text{fit}} &= 0.30 \text{ (nV/V)/\% (1000 N}\cdot\text{m)} \\ u(e_T)_{\text{fit}} &= 0.16 \text{ (nV/V)/K (500 N}\cdot\text{m)} & u(e_T)_{\text{fit}} &= 0.34 \text{ (nV/V)/K (1000 N}\cdot\text{m)} \\ \text{TT1:} \quad u(e_{rH})_{\text{fit}} &= 1.10 \text{ (nV/V)/\% (500 N}\cdot\text{m)} & u(e_{rH})_{\text{fit}} &= 2.50 \text{ (nV/V)/\% (1000 N}\cdot\text{m)} \\ u(e_T)_{\text{fit}} &= 1.25 \text{ (nV/V)/K (500 N}\cdot\text{m)} & u(e_T)_{\text{fit}} &= 2.84 \text{ (nV/V)/K (1000 N}\cdot\text{m)}. \end{aligned} \quad (10)$$

the following standard uncertainties resulted

TB2 :	$u(e_{rH}) = 0.25 \text{ (nV/V)/\% (500 N}\cdot\text{m)}$	$u(e_{rH}) = 0.38 \text{ (nV/V)/\% (1000 N}\cdot\text{m)}$	(11)
	$u(e_T) = 0.32 \text{ (nV/V)/K (500 N}\cdot\text{m)}$	$u(e_T) = 0.50 \text{ (nV/V)/K (1000 N}\cdot\text{m)}$	
TT1 :	$u(e_{rH}) = 1.24 \text{ (nV/V)/\% (500 N}\cdot\text{m)}$	$u(e_{rH}) = 2.76 \text{ (nV/V)/\% (1000 N}\cdot\text{m)}$	
	$u(e_T) = 1.34 \text{ (nV/V)/K (500 N}\cdot\text{m)}$	$u(e_T) = 3.04 \text{ (nV/V)/K (1000 N}\cdot\text{m)}$	

The expanded uncertainties are given in table 5.

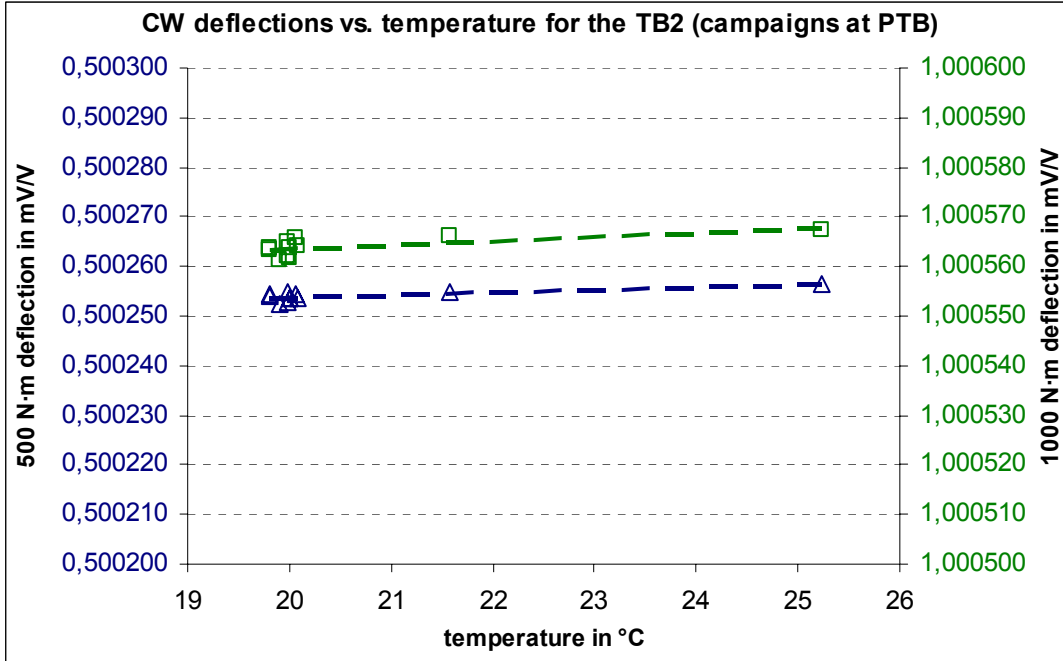


Figure 7. Clockwise deflections in mV/V of the TB2 measured during campaigns at the pilot laboratory vs. temperature: for 500 N·m (triangles, left axis of ordinates) and 1000 N·m (squares, right axis of ordinates), scaling range: 100 nV/V, humidity influence corrected

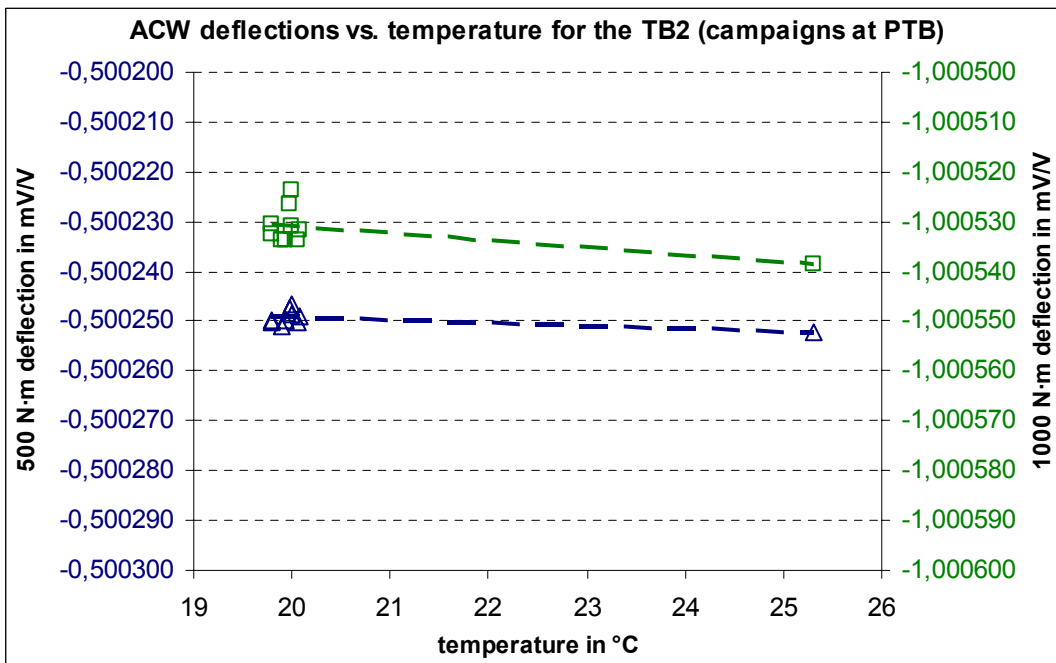


Figure 8. Anti-clockwise deflections in mV/V of the TB2 measured during campaigns at the pilot laboratory vs. temperature: for 500 N·m (triangles, left axis of ordinates) and 1000 N·m (squares, right axis of ordinates), scaling range: 100 nV/V, humidity influence corrected

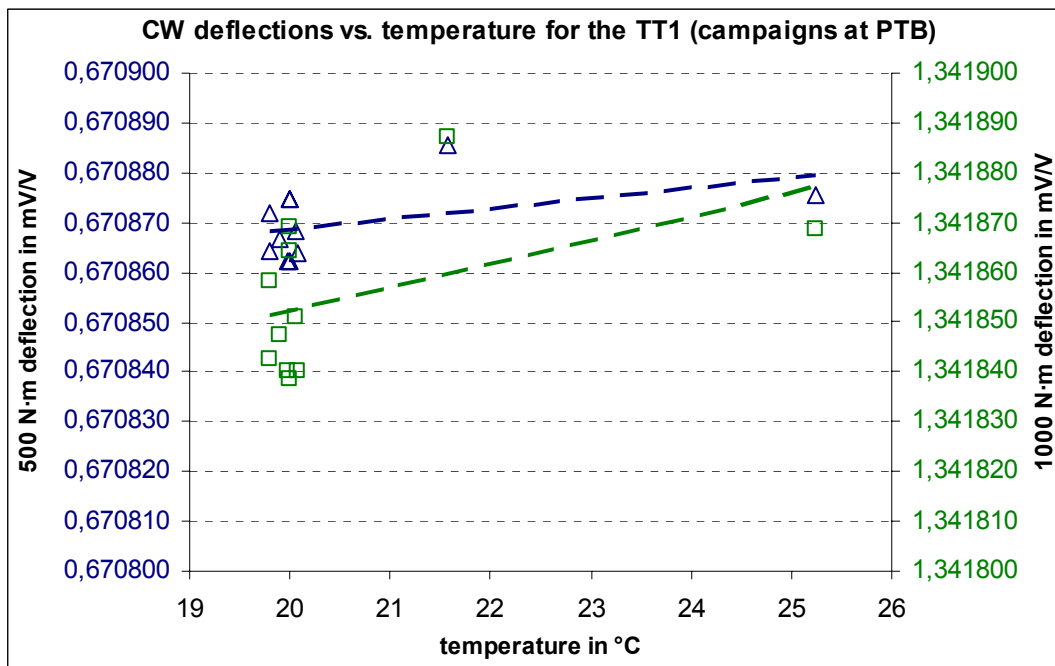


Figure 9. Clockwise deflections in mV/V of the TT1 measured during campaigns at the pilot laboratory vs. temperature: for 500 N·m (triangles, left axis of ordinates) and 1000 N·m (squares, right axis of ordinates), scaling range: 100 nV/V, humidity influence corrected

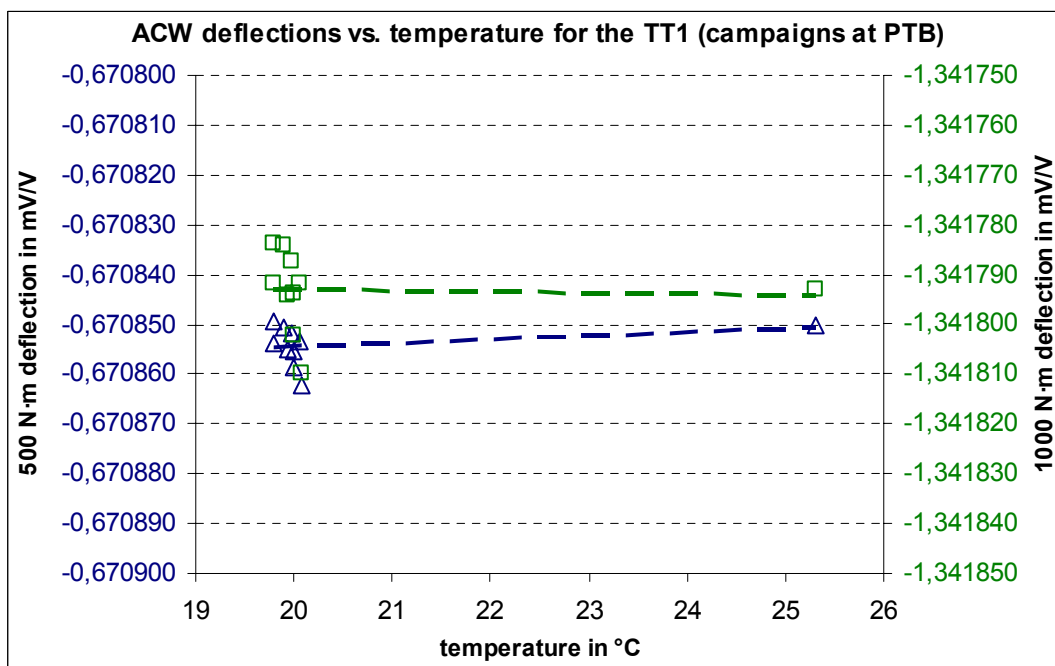


Figure 10. Anti-clockwise deflections in mV/V of the TT1 measured during campaigns at the pilot laboratory vs. temperature: for 500 N·m (triangles, left axis of ordinates) and 1000 N·m (squares, right axis of ordinates), scaling range: 100 nV/V, humidity influence corrected

Table 5: Calculated humidity e_{RH} and temperature e_T coefficients of the transfer transducers (from measurements only in clockwise direction)

	500 N·m	1000 N·m	-500 N·m	-1000 N·m
Air humidity coefficient and expanded uncertainty ($k = 2$) in (nV/V)/%				
TB2, S/N #044430025/1 kN·m	0.2 ± 0.5	0.2 ± 0.8	-0.2 ± 0.5	-0.2 ± 0.8
TT1, S/N 36079-00	-2.5 ± 2.5	-5.1 ± 5.5	2.5 ± 2.5	5.1 ± 5.5
Temperature coefficient and expanded uncertainty ($k = 2$) in (nV/V)/K				
TB2, S/N #044430025/1 kN·m	0.5 ± 0.6	0.8 ± 1.0	-0.5 ± 0.6	-0.8 ± 1.0
TT1, S/N 36079-00	0.4 ± 2.7	1.5 ± 6.1	-0.4 ± 2.7	-1.5 ± 6.1

The figures 11 to 18 show the environmental conditions (temperature and humidity of the ambient air) in the participating labs as recorded by the data logger Hobo. These values were taken to calculate the corrected results in table 10 (except for participant A, because the Hobo had not been placed near the transducers during the measurement there leading to higher deviations of the indications from the local conditions – the local values were used instead). The Hobo is not a very accurate temperature and humidity measuring instrument in terms of absolute values. But it is stable enough in order to get better comparable values for the environmental conditions. The date and time shown in the diagrams is the local time in the pilot laboratory. The time difference between pilot and participant is not taken into account.

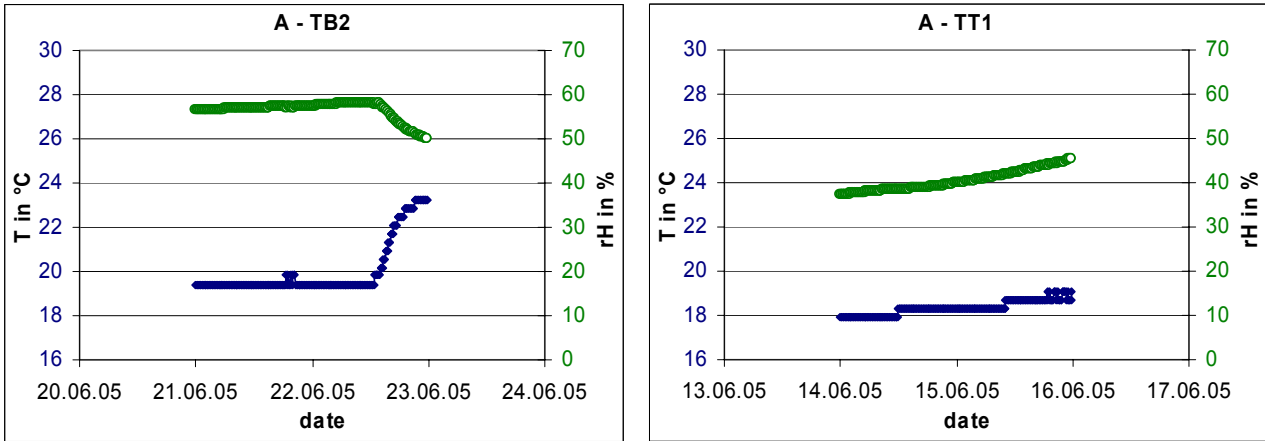


Figure 11. Environmental conditions during the calibration of the TB2 (left diagram) and the TT1 (right diagram) by participant A (full symbol - temperature on left ordinate, empty symbol - relative humidity on right ordinate). The localized values are $T = 20.2^{\circ}\text{C}$, $rH = 48\%$ over the whole period.

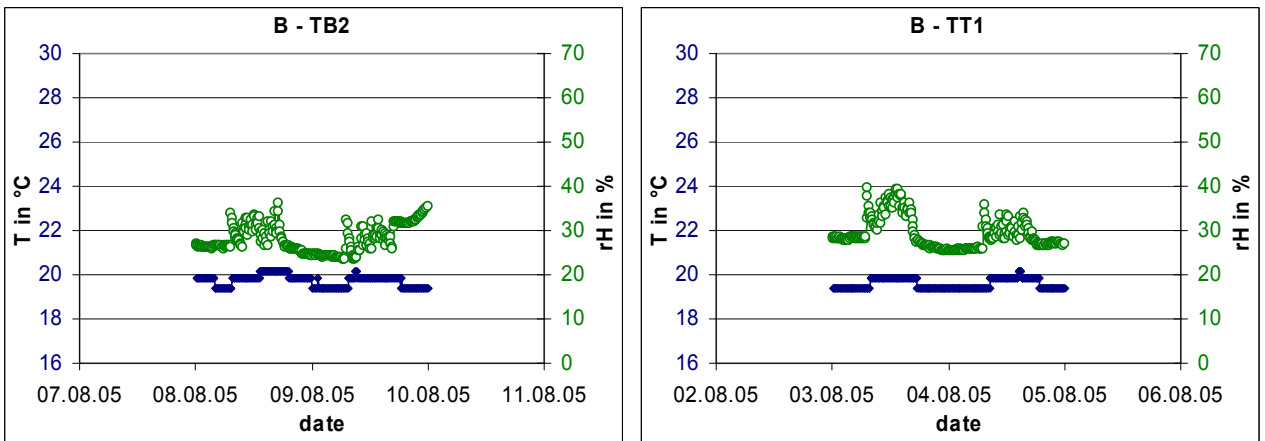


Figure 12. Environmental conditions during the calibration of the TB2 (left diagram) and the TT1 (right diagram) by participant B (full symbol - temperature on left ordinate, empty symbol - relative humidity on right ordinate)

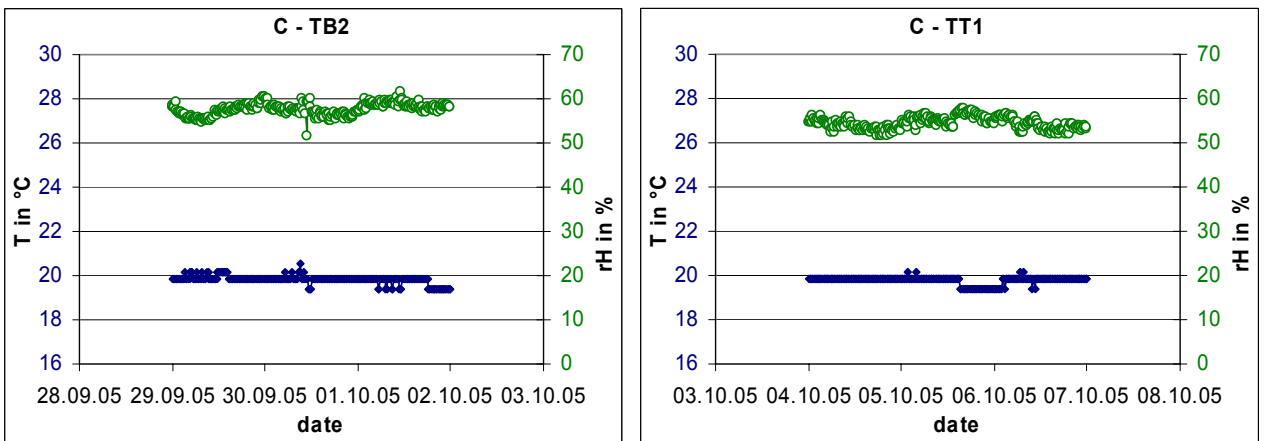


Figure 13. Environmental conditions during the calibration of the TB2 (left diagram) and the TT1 (right diagram) by participant C (full symbol - temperature on left ordinate, empty symbol - relative humidity on right ordinate)

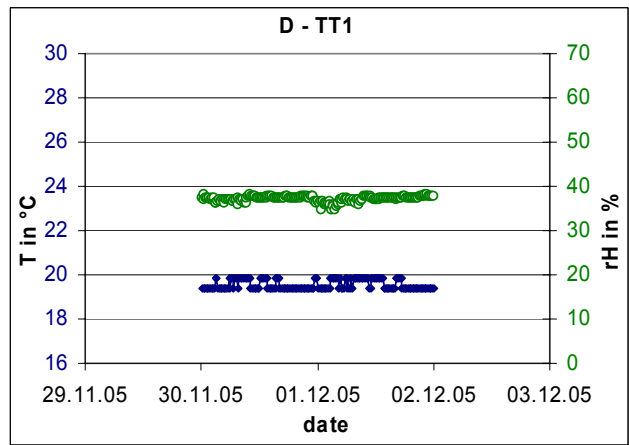
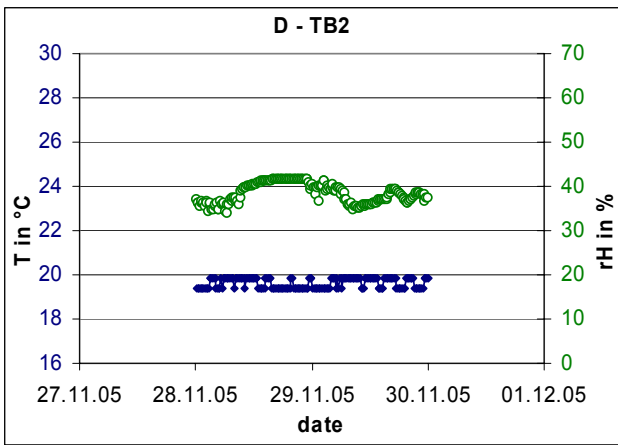


Figure 14. Environmental conditions during the calibration of the TB2 (left diagram) and the TT1 (right diagram) by participant D (full symbol - temperature on left ordinate, empty symbol - relative humidity on right ordinate)

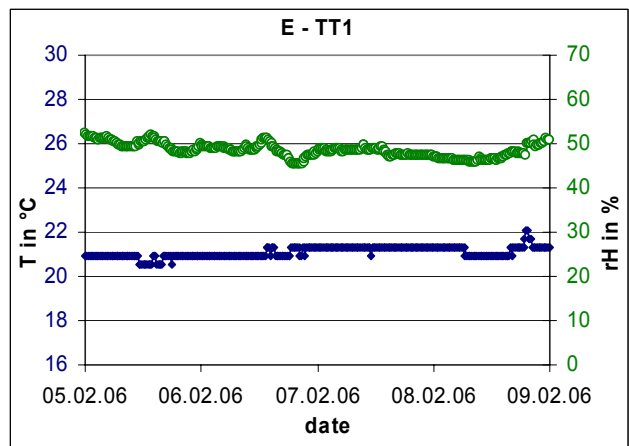
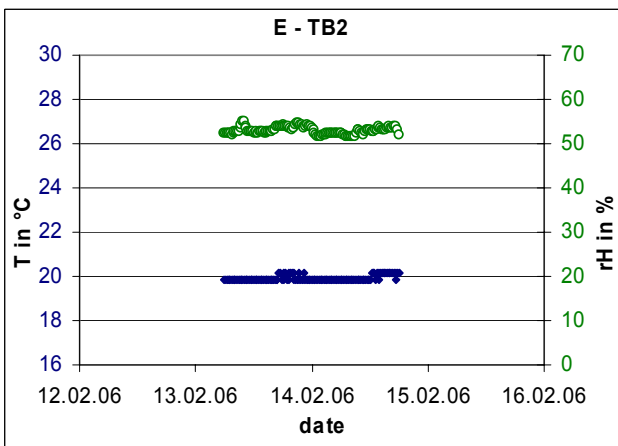


Figure 15. Environmental conditions during the calibration of the TB2 (left diagram) and the TT1 (right diagram) by participant E (full symbol - temperature on left ordinate, empty symbol - relative humidity on right ordinate)

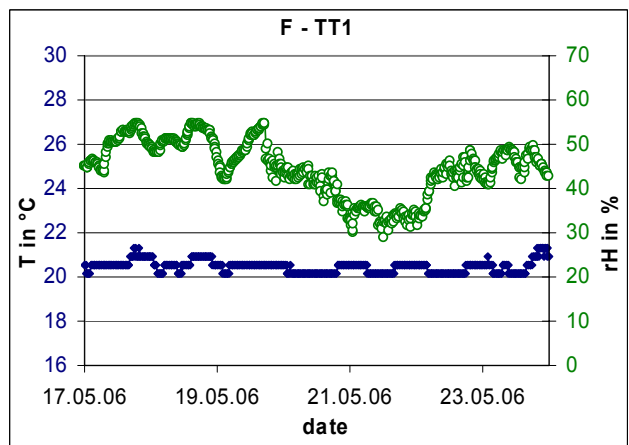
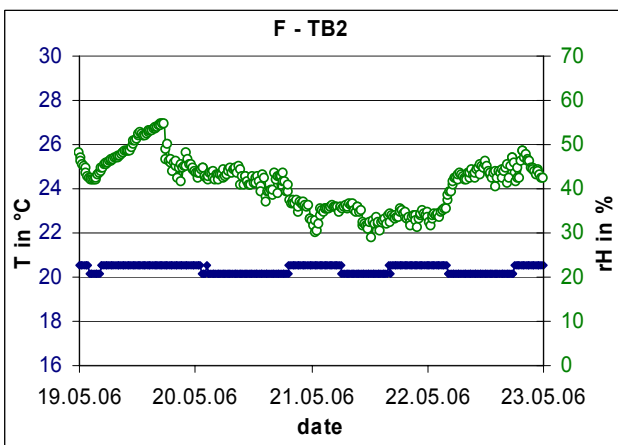


Figure 16. Environmental conditions during the calibration of the TB2 (left diagram) and the TT1 (right diagram) by participant F (full symbol - temperature on left ordinate, empty symbol - relative humidity on right ordinate)

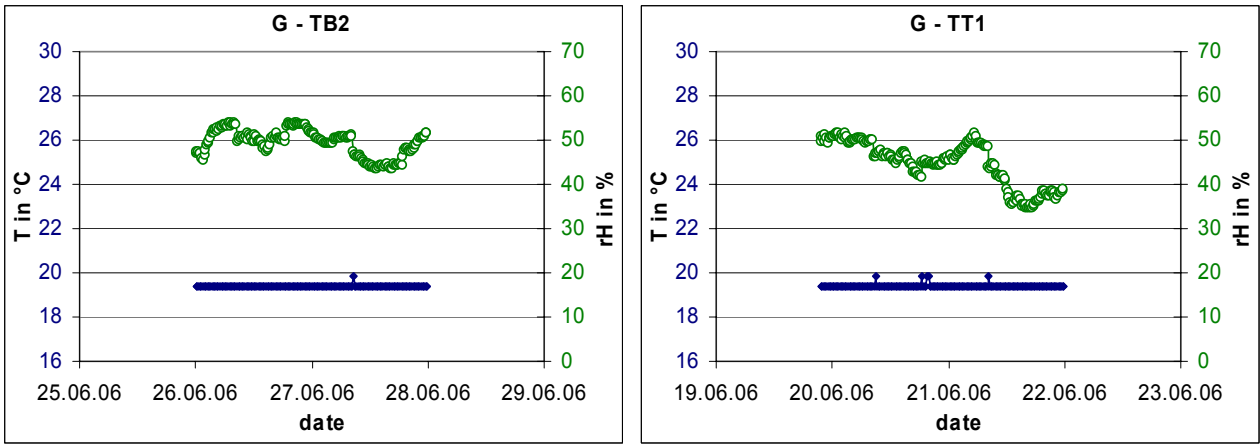


Figure 17. Environmental conditions during the calibration of the TB2 (left diagram) and the TT1 (right diagram) by participant G (full symbol - temperature on left ordinate, empty symbol - relative humidity on right ordinate)

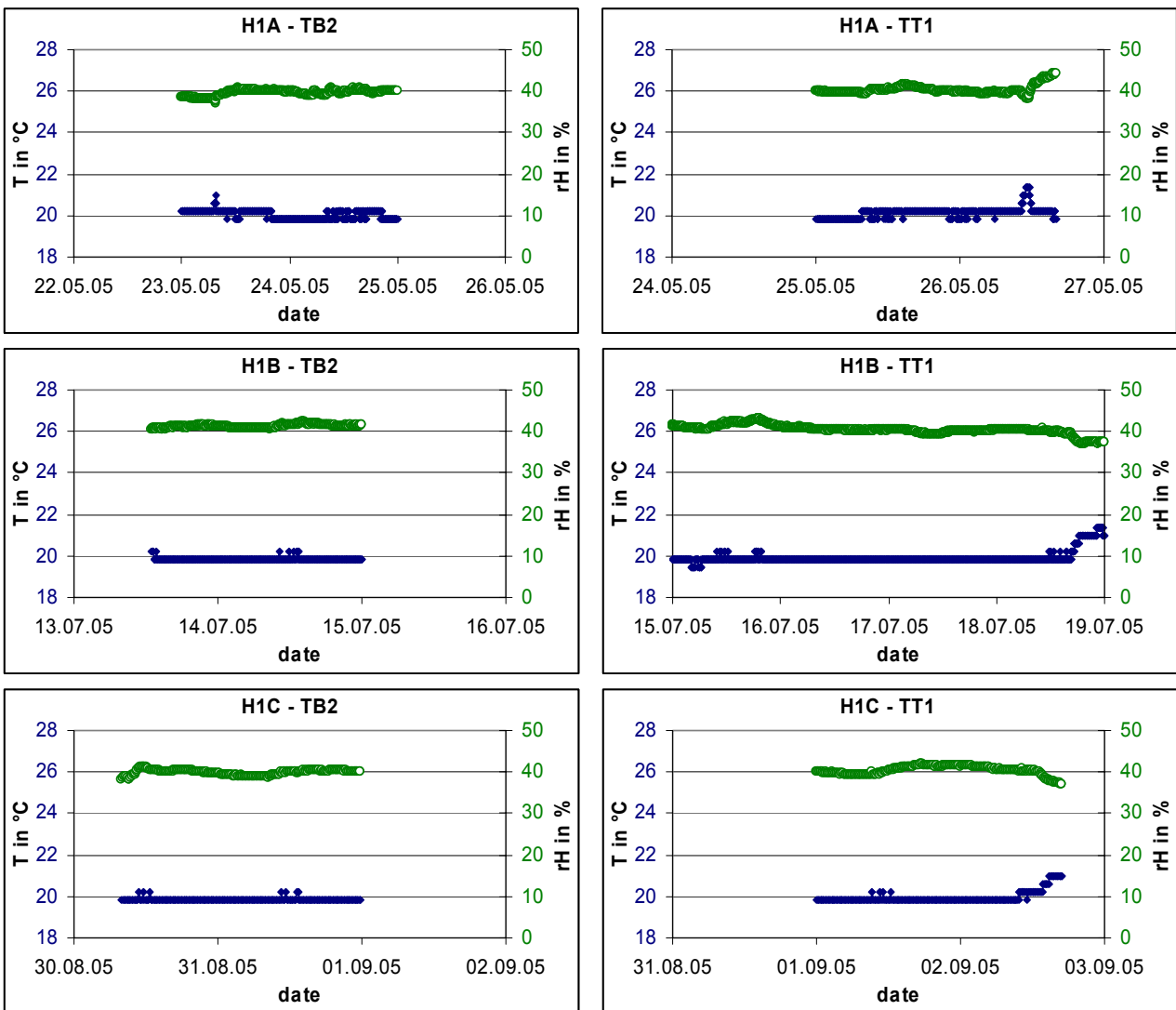


Figure 18. Environmental conditions during the calibration of the TB2 (left diagram) and the TT1 (right diagram) by participant H (full symbol - temperature on left ordinate, empty symbol - relative humidity on right ordinate) for the first three measuring campaigns (H1A, H1B and H1C)

Using the values e_{rH} and e_T given in table 5, for each of the participants the deflections can be corrected taking into account the corresponding deviations Δ from the ideal environmental conditions ($T = 20^\circ\text{C}$, $rH = 40\%$) according to (12):

$$Y_i^m = Y_i^n - e_{rH} \cdot \Delta rH - e_T \cdot \Delta T \quad (12)$$

with Y_i'' being the uncorrected and Y_i''' the corrected deflections.

Stability of the transfer transducers

a) Stability of the sensitivity over the complete period of the key comparison

Based on the fact that the quality of the comparison substantially depends on the three measurements during the loop, the stability of the transducers is extremely important. The figures 19 to 26 show the stability of the transducers, which is determined as the relative deviations of the resulting deflections for all measurements made by the pilot from their arithmetical mean value. The chronological order of the calibrations in the pilot and the participating laboratories is given in table 6.

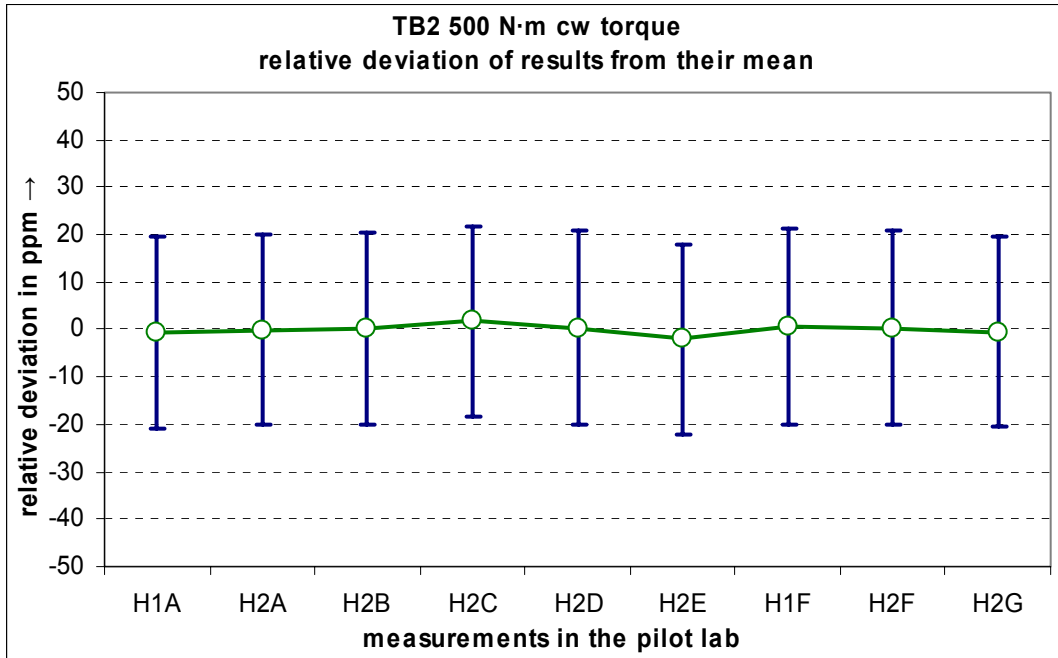


Figure 19. Relative deviations of the deflections for all measurements made by the pilot from their mean value (0.500254 mV/V) for transducer TB2 at 500 N·m clockwise torque and relative expanded ($k = 2$) measurement uncertainties (uncertainty bars), values corrected for the influence of temperature and humidity

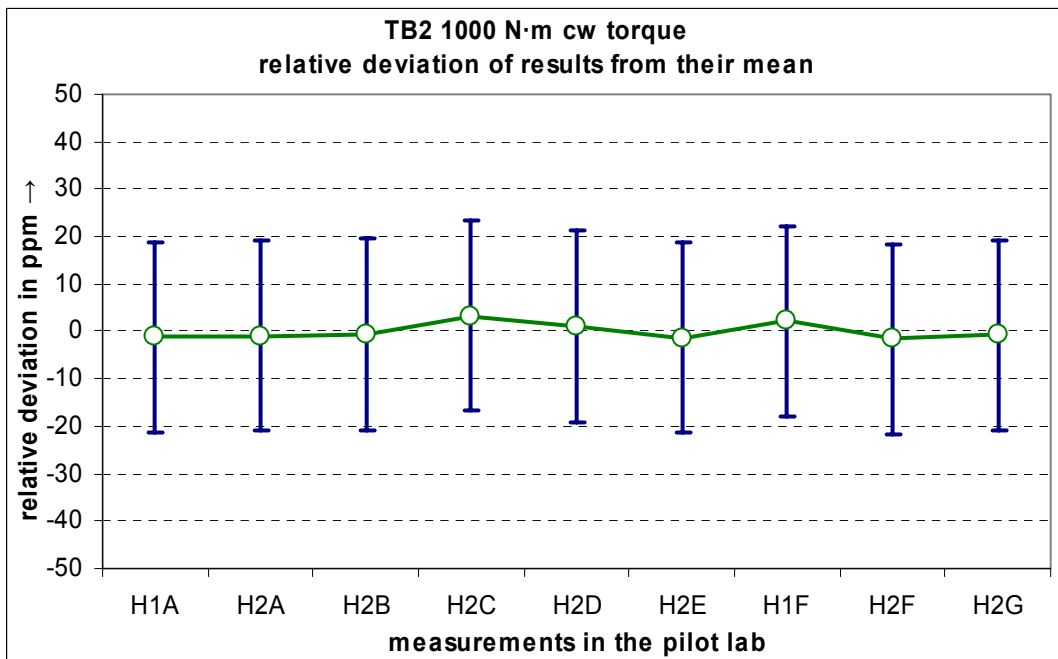


Figure 20. Relative deviations of the deflections for all measurements made by the pilot from their mean value (1.000565 mV/V) for transducer TB2 at 1000 N·m clockwise torque and relative expanded ($k = 2$) measurement uncertainties (uncertainty bars), values corrected for the influence of temperature and humidity

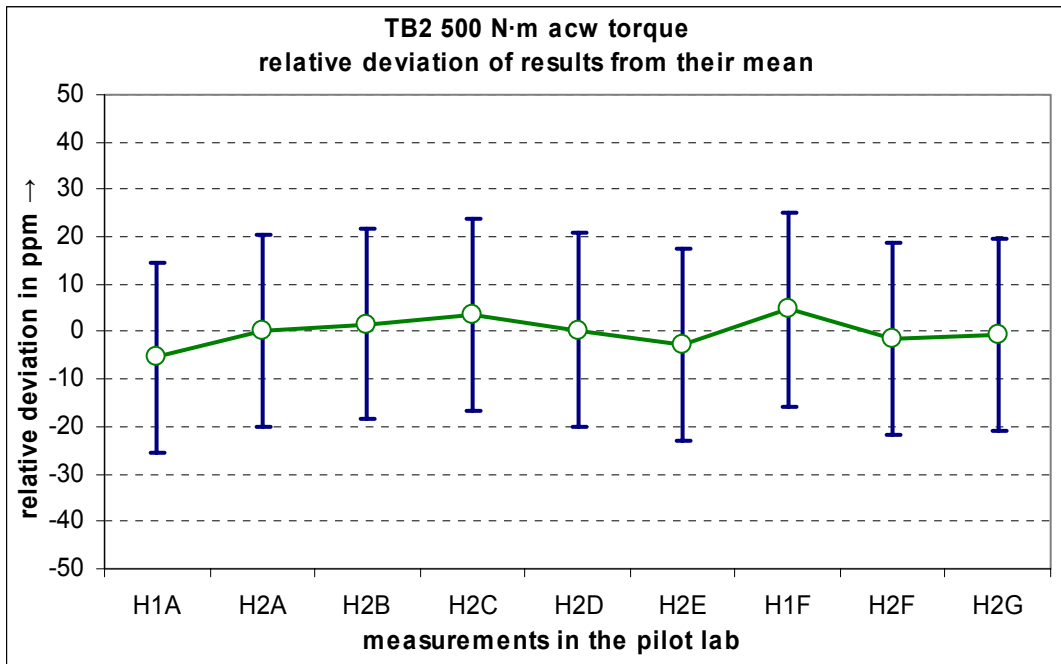


Figure 21. Relative deviations of the deflections for all measurements made by the pilot from their mean value (-0.500249 mV/V) for transducer TB2 at 500 N·m anti-clockwise torque and relative expanded ($k=2$) measurement uncertainties (uncertainty bars), values corrected for the influence of temperature and humidity

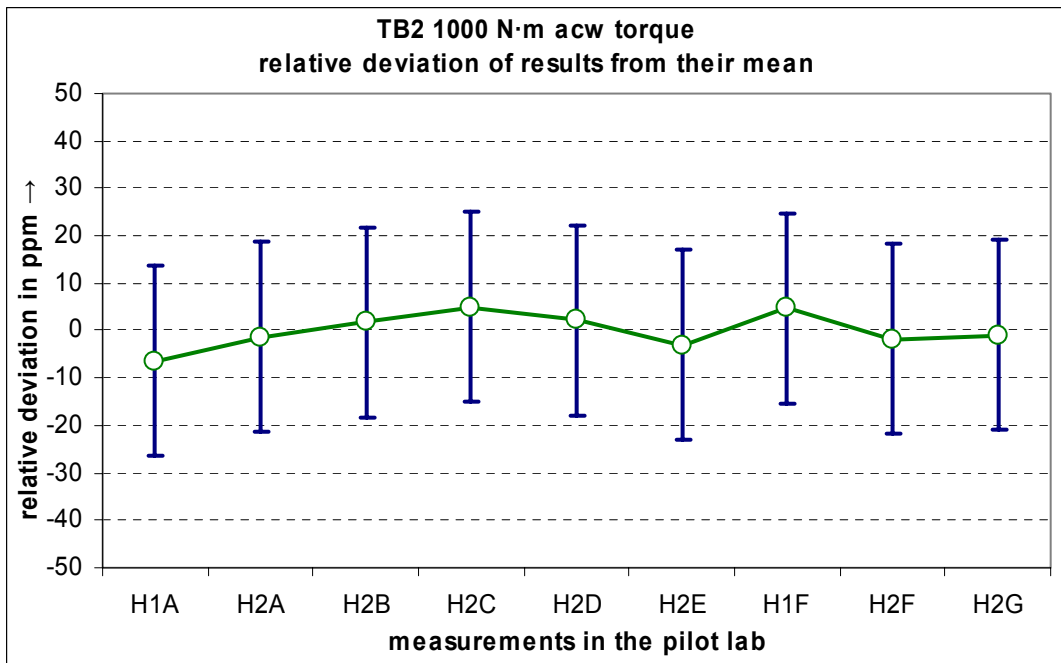


Figure 22. Relative deviations of the deflections for all measurements made by the pilot from their mean value (-1.000530 mV/V) for transducer TB2 at 1000 N·m anti-clockwise torque and relative expanded ($k=2$) measurement uncertainties (uncertainty bars), values corrected for the influence of temperature and humidity

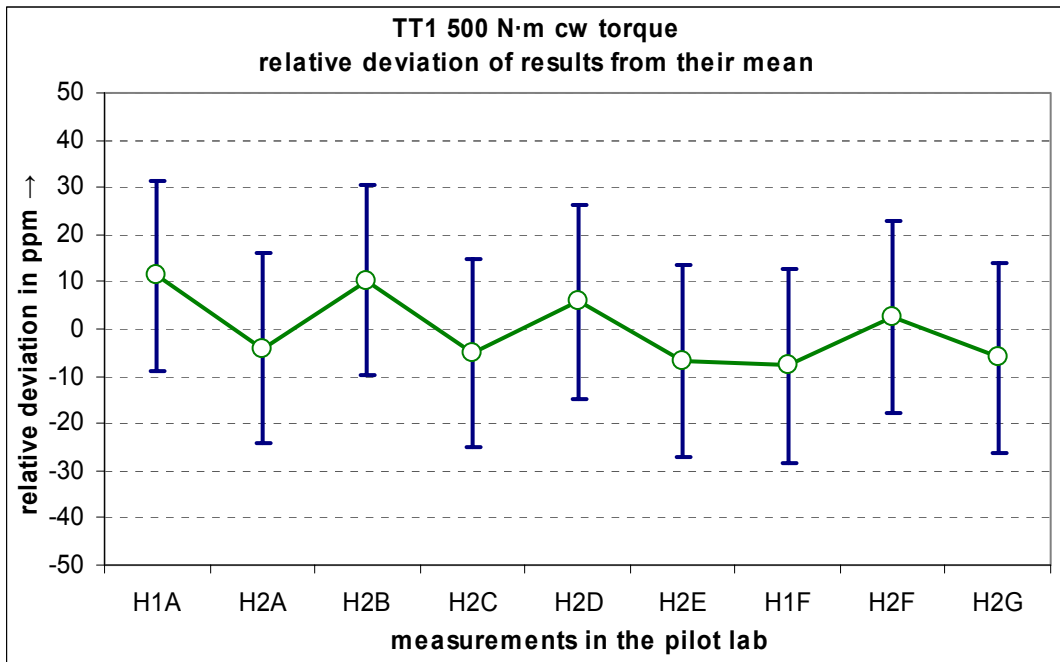


Figure 23. Relative deviations of the deflections for all measurements made by the pilot from their mean value (0.670868 mV/V) for transducer TT1 at 500 N·m clockwise torque and relative expanded ($k = 2$) measurement uncertainties (uncertainty bars), values corrected for the influence of temperature and humidity

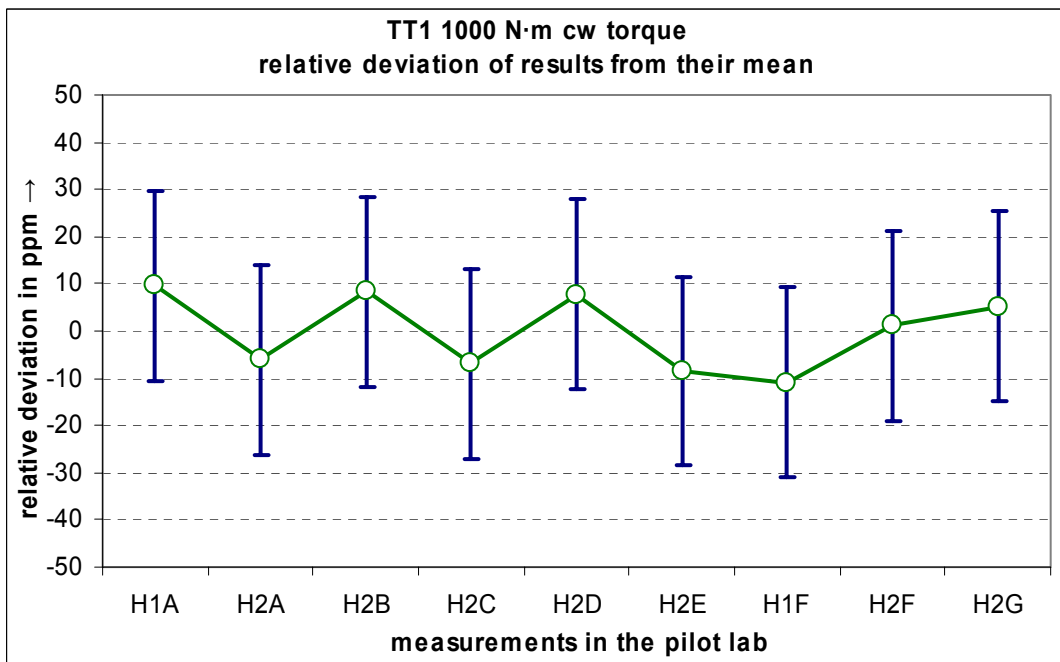


Figure 24. Relative deviations of the deflections for all measurements made by the pilot from their mean value (1.341852 mV/V) for transducer TT1 at 1000 N·m clockwise torque and relative expanded ($k = 2$) measurement uncertainties (uncertainty bars), values corrected for the influence of temperature and humidity

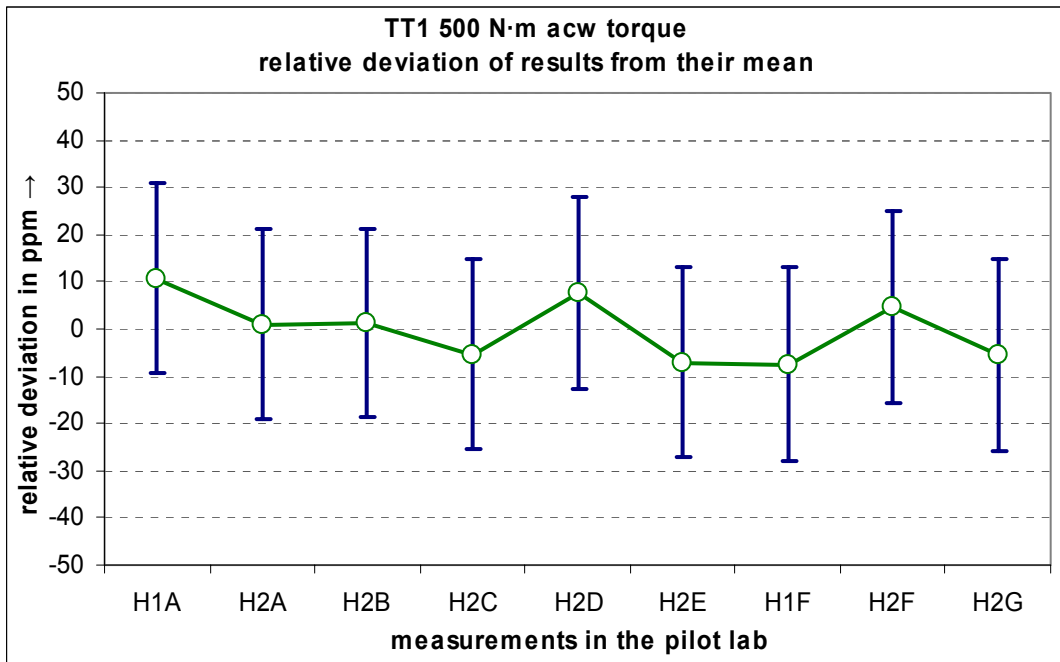


Figure 25. Relative deviations of the deflections for all measurements made by the pilot from their mean value (-0.670852 mV/V) for transducer TT1 at 500 N·m anti-clockwise torque and relative expanded ($k = 2$) measurement uncertainties (uncertainty bars), values corrected for the influence of temperature and humidity

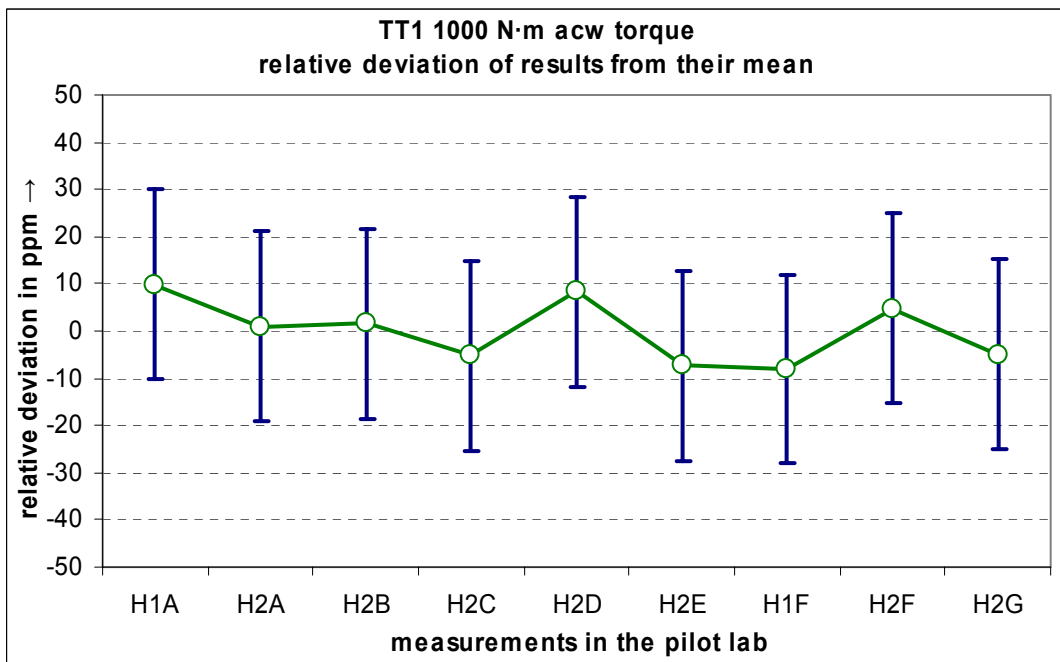


Figure 26. Relative deviations of the deflections for all measurements made by the pilot from their mean value (-1.341787 mV/V) for transducer TT1 at 1000 N·m anti-clockwise torque and relative expanded ($k = 2$) measurement uncertainties (uncertainty bars), values corrected for the influence of temperature and humidity

Table 6: Chronological order of the calibrations during the key comparison

Measurement	TB2		TT1	
	clockwise	anti- clockwise	clockwise	anti- clockwise
H1A	23.05.2005	24.05.2005	25.05.2005	26.05.2005
A	21.06.2005	22.06.2005	21.06.2005	22.06.2005
H2A H1B	13.07.2005	14.07.2005	15.07.2005	18.07.2005
B	08.08.2005	09.08.2005	03.08.2005	04.08.2005
H2B H1C	30.08.2005	31.08.2005	01.09.2005	02.09.2005
C	29.09.2005	01.10.2005	06.10.2005	04.10.2005
H2C H1D	01.11.2005	02.11.2005	03.11.2005	04.11.2005
D	28.11.2005	29.11.2005	30.11.2005	01.12.2005
H2D H1E	19.12.2005	20.12.2005	21.12.2005	22.12.2005
E	14.02.2006	13.02.2006	05.02.2006	08.02.2006
H2E	06.03.2006	07.03.2006	08.03.2006	09.03.2006
H1F	11.04.2006	11.04.2006	12.04.2006	13.04.2006
F	19.05.2006	22.05.2006	17.05.2006	23.05.2006
H2F H1G	08.06.2006	09.06.2006	12.06.2006	13.06.2006
G	27.06.2006	26.06.2006	20.06.2006	21.06.2006
H2G	10.07.2006	11.07.2006	12.07.2006	13.07.2006

b) Stability in the loops

The measurements in the pilot laboratory (see figures 11 to 18) demonstrate that the stability of the travelling standards is sufficiently good compared with the uncertainty of measurement and there is no evidence for a drift. The deviations from the mean show a stochastic behaviour. Therefore it was not necessary to use drift corrections for the results from the participants in the different loops. That means, that the single loops don't need to be considered as independent of each other and their numerical (corrected) values can be compared. However, a correction for the different environmental conditions in the participating laboratories has to be used to calculate the results.

7. Results of the measurements: reported deflections and uncertainties, calculated corrections

All results are given in the tables in section 7.1: the deflections as reported by the participants and the values with

- corrections for the amplifier according to 5, equation (1), additionally
- corrections for the creep influence due to different loading regimes in the machines according to 6 (section "Creep effect"), equation (2), and - also in addition -
- corrections for the environmental conditions according to 6 (section "Humidity and temperature influences on the sensitivity") , equation (12).

The pilot reports the arithmetical mean of all measurements made in this laboratory and the arithmetical mean of the corresponding corrected values.

The calculation of the weighted means and the key comparison reference values (KCRV) as well as the χ^2 tests are given in the annex A.1 according to procedure A in [3]. The parts A.2 and A.3 contain the calculation of the relative deviations of the deflections from the corresponding KCRV and of the degrees of equivalence.

The following designations are used in the tables 7 to 10:

Y_{P-Rep} (= Y_i) Deflection reported by participant P (for the pilot: mean of all measurements), in mV/V

Y_{P-DMP} (= Y_i') Deflection for participant P, corrected for the influence of the DMP40, in mV/V

$Y_{P-Creep}$ (= Y_i'') Deflection for participant P, additionally corrected for the creep influence, in mV/V

$Y_{P-Envir}$ (= Y_i''') Deflection for participant P, additionally corrected for the environmental influence, in mV/V

W_{P-Rep} = Expanded relative uncertainty ($k = 2$) of Y_{P-Rep} (for the pilot: mean of all measurements)

W_{P-DMP} = Expanded relative uncertainty ($k = 2$) of Y_{P-DMP}

$W_{P-Creep}$ = Expanded relative uncertainty ($k = 2$) of $Y_{P-Creep}$

$W_{P-Envir}$ = Expanded relative uncertainty ($k = 2$) of $Y_{P-Envir}$

Table 7: Uncorrected deflections in mV/V and expanded relative uncertainties ($k = 2$) as reported by the participants

Participant	TB2 - clockwise torque				TT1 - clockwise torque			
	500 N·m		1000 N·m		500 N·m		1000 N·m	
	Y_{P-Rep}	W_{P-Rep}	Y_{P-Rep}	W_{P-Rep}	Y_{P-Rep}	W_{P-Rep}	Y_{P-Rep}	W_{P-Rep}
A	0.500270	$4.1 \cdot 10^{-5}$	1.000605	$4.0 \cdot 10^{-5}$	0.670857	$4.0 \cdot 10^{-5}$	1.341843	$4.0 \cdot 10^{-5}$
B	0.500253	$2.1 \cdot 10^{-5}$	1.000569	$2.0 \cdot 10^{-5}$	0.670922	$2.0 \cdot 10^{-5}$	1.341961	$2.0 \cdot 10^{-5}$
C	0.500278	$3.0 \cdot 10^{-5}$	1.000618	$3.0 \cdot 10^{-5}$	0.670797	$3.0 \cdot 10^{-5}$	1.341701	$3.0 \cdot 10^{-5}$
D	0.500269	$4.9 \cdot 10^{-5}$	1.000602	$4.9 \cdot 10^{-5}$	0.670893	$4.9 \cdot 10^{-5}$	1.341914	$4.9 \cdot 10^{-5}$
E	0.500252	$1.0 \cdot 10^{-4}$	1.000567	$1.0 \cdot 10^{-4}$	0.670816	$1.0 \cdot 10^{-4}$	1.341744	$1.0 \cdot 10^{-4}$
F	0.500256	$5.5 \cdot 10^{-5}$	1.000601	$4.3 \cdot 10^{-5}$	0.670812	$4.6 \cdot 10^{-5}$	1.341760	$4.3 \cdot 10^{-5}$
G	0.500256	$2.3 \cdot 10^{-5}$	1.000571	$2.1 \cdot 10^{-5}$	0.670826	$2.2 \cdot 10^{-5}$	1.341763	$2.0 \cdot 10^{-5}$
H	0.500256	$2.0 \cdot 10^{-5}$	1.000566	$2.0 \cdot 10^{-5}$	0.670869	$2.1 \cdot 10^{-5}$	1.341850	$2.0 \cdot 10^{-5}$
Participant	TB2 - anti-clockwise torque				TT1 - anti-clockwise torque			
	-500 N·m		-1000 N·m		-500 N·m		-1000 N·m	
	Y_{P-Rep}	W_{P-Rep}	Y_{P-Rep}	W_{P-Rep}	Y_{P-Rep}	W_{P-Rep}	Y_{P-Rep}	W_{P-Rep}
A	-0.500243	$4.0 \cdot 10^{-5}$	-1.000544	$4.0 \cdot 10^{-5}$	-0.670811	$4.0 \cdot 10^{-5}$	-1.341734	$4.0 \cdot 10^{-5}$
B	-0.500243	$2.0 \cdot 10^{-5}$	-1.000532	$2.0 \cdot 10^{-5}$	-0.670912	$2.1 \cdot 10^{-5}$	-1.341911	$2.0 \cdot 10^{-5}$
C	-0.500269	$3.0 \cdot 10^{-5}$	-1.000589	$3.0 \cdot 10^{-5}$	-0.670773	$3.0 \cdot 10^{-5}$	-1.341632	$3.0 \cdot 10^{-5}$
D	-0.500256	$5.0 \cdot 10^{-5}$	-1.000561	$4.9 \cdot 10^{-5}$	-0.670876	$4.9 \cdot 10^{-5}$	-1.341844	$4.9 \cdot 10^{-5}$
E	-0.500247	$1.0 \cdot 10^{-4}$	-1.000536	$1.0 \cdot 10^{-4}$	-0.670799	$1.0 \cdot 10^{-4}$	-1.341688	$1.0 \cdot 10^{-4}$
F	-0.500291	$5.2 \cdot 10^{-5}$	-1.000657	$4.6 \cdot 10^{-5}$	-0.670890	$4.1 \cdot 10^{-5}$	-1.341844	$4.1 \cdot 10^{-5}$
G	-0.500260	$2.1 \cdot 10^{-5}$	-1.000571	$2.1 \cdot 10^{-5}$	-0.670856	$2.2 \cdot 10^{-5}$	-1.341803	$2.2 \cdot 10^{-5}$
H	-0.500248	$2.0 \cdot 10^{-5}$	-1.000532	$2.0 \cdot 10^{-5}$	-0.670851	$2.0 \cdot 10^{-5}$	-1.341785	$2.0 \cdot 10^{-5}$

Table 8: Deflections from table 7 in mV/V, corrected for the influence of the DMP40, and corresponding expanded relative uncertainties ($k = 2$)

Participant	TB2 - clockwise torque				TT1 - clockwise torque			
	500 N·m		1000 N·m		500 N·m		1000 N·m	
	Y_{P-DMP}	W_{P-DMP}	Y_{P-DMP}	W_{P-DMP}	Y_{P-DMP}	W_{P-DMP}	Y_{P-DMP}	W_{P-DMP}
A	0.500266	$4.1 \cdot 10^{-5}$	1.000598	$4.1 \cdot 10^{-5}$	0.670853	$4.1 \cdot 10^{-5}$	1.341836	$4.1 \cdot 10^{-5}$
B	0.500251	$2.1 \cdot 10^{-5}$	1.000564	$2.2 \cdot 10^{-5}$	0.670918	$2.1 \cdot 10^{-5}$	1.341954	$2.2 \cdot 10^{-5}$
C	0.500277	$3.1 \cdot 10^{-5}$	1.000617	$3.1 \cdot 10^{-5}$	0.670795	$3.1 \cdot 10^{-5}$	1.341697	$3.1 \cdot 10^{-5}$
D	0.500272	$5.0 \cdot 10^{-5}$	1.000605	$5.0 \cdot 10^{-5}$	0.670892	$5.0 \cdot 10^{-5}$	1.341914	$5.0 \cdot 10^{-5}$
E	0.500249	$1.0 \cdot 10^{-4}$	1.000568	$1.0 \cdot 10^{-4}$	0.670815	$1.0 \cdot 10^{-4}$	1.341741	$1.0 \cdot 10^{-4}$
F	0.500253	$5.5 \cdot 10^{-5}$	1.000602	$4.4 \cdot 10^{-5}$	0.670810	$4.6 \cdot 10^{-5}$	1.341759	$4.4 \cdot 10^{-5}$
G	0.500255	$2.4 \cdot 10^{-5}$	1.000569	$2.2 \cdot 10^{-5}$	0.670825	$2.2 \cdot 10^{-5}$	1.341762	$2.2 \cdot 10^{-5}$
H	0.500254	$2.1 \cdot 10^{-5}$	1.000564	$2.2 \cdot 10^{-5}$	0.670868	$2.1 \cdot 10^{-5}$	1.341850	$2.2 \cdot 10^{-5}$
Participant	TB2 - anti-clockwise torque				TT1 - anti-clockwise torque			
	-500 N·m		-1000 N·m		-500 N·m		-1000 N·m	
	Y_{P-DMP}	W_{P-DMP}	Y_{P-DMP}	W_{P-DMP}	Y_{P-DMP}	W_{P-DMP}	Y_{P-DMP}	W_{P-DMP}
A	-0.500240	$4.1 \cdot 10^{-5}$	-1.000537	$4.1 \cdot 10^{-5}$	-0.670806	$4.1 \cdot 10^{-5}$	-1.341729	$4.1 \cdot 10^{-5}$
B	-0.500241	$2.1 \cdot 10^{-5}$	-1.000526	$2.2 \cdot 10^{-5}$	-0.670910	$2.1 \cdot 10^{-5}$	-1.341906	$2.2 \cdot 10^{-5}$
C	-0.500270	$3.1 \cdot 10^{-5}$	-1.000587	$3.1 \cdot 10^{-5}$	-0.670771	$3.1 \cdot 10^{-5}$	-1.341633	$3.1 \cdot 10^{-5}$
D	-0.500256	$5.0 \cdot 10^{-5}$	-1.000558	$5.0 \cdot 10^{-5}$	-0.670876	$5.0 \cdot 10^{-5}$	-1.341840	$5.0 \cdot 10^{-5}$
E	-0.500243	$1.0 \cdot 10^{-4}$	-1.000537	$1.0 \cdot 10^{-4}$	-0.670801	$1.0 \cdot 10^{-4}$	-1.341685	$1.0 \cdot 10^{-4}$
F	-0.500293	$5.2 \cdot 10^{-5}$	-1.000653	$4.6 \cdot 10^{-5}$	-0.670892	$4.1 \cdot 10^{-5}$	-1.341843	$4.2 \cdot 10^{-5}$
G	-0.500261	$2.1 \cdot 10^{-5}$	-1.000570	$2.2 \cdot 10^{-5}$	-0.670852	$2.2 \cdot 10^{-5}$	-1.341800	$2.3 \cdot 10^{-5}$
H	-0.500249	$2.1 \cdot 10^{-5}$	-1.000531	$2.2 \cdot 10^{-5}$	-0.670851	$2.1 \cdot 10^{-5}$	-1.341787	$2.2 \cdot 10^{-5}$

Table 9: Deflections from table 8 in mV/V, additionally corrected for the influence of the creep, and corresponding expanded relative uncertainties ($k = 2$)

Participant	TB2 - clockwise torque				TT1 - clockwise torque			
	500 N·m		1000 N·m		500 N·m		1000 N·m	
	$Y_{P-Creep}$	$W_{P-Creep}$	$Y_{P-Creep}$	$W_{P-Creep}$	$Y_{P-Creep}$	$W_{P-Creep}$	$Y_{P-Creep}$	$W_{P-Creep}$
A	0.500266	$4.1 \cdot 10^{-5}$	1.000598	$4.1 \cdot 10^{-5}$	0.670853	$4.1 \cdot 10^{-5}$	1.341836	$4.1 \cdot 10^{-5}$
B	0.500251	$2.1 \cdot 10^{-5}$	1.000564	$2.2 \cdot 10^{-5}$	0.670918	$2.1 \cdot 10^{-5}$	1.341954	$2.2 \cdot 10^{-5}$
C	0.500277	$3.1 \cdot 10^{-5}$	1.000617	$3.1 \cdot 10^{-5}$	0.670795	$3.1 \cdot 10^{-5}$	1.341697	$3.1 \cdot 10^{-5}$
D	0.500274	$5.1 \cdot 10^{-5}$	1.000607	$5.0 \cdot 10^{-5}$	0.670895	$5.1 \cdot 10^{-5}$	1.341917	$5.0 \cdot 10^{-5}$
E	0.500252	$1.0 \cdot 10^{-4}$	1.000571	$1.0 \cdot 10^{-4}$	0.670819	$1.0 \cdot 10^{-4}$	1.341745	$1.0 \cdot 10^{-4}$
F	0.500254	$5.6 \cdot 10^{-5}$	1.000603	$4.4 \cdot 10^{-5}$	0.670812	$4.6 \cdot 10^{-5}$	1.341761	$4.4 \cdot 10^{-5}$
G	0.500256	$2.4 \cdot 10^{-5}$	1.000570	$2.2 \cdot 10^{-5}$	0.670826	$2.3 \cdot 10^{-5}$	1.341764	$2.2 \cdot 10^{-5}$
H	0.500254	$2.1 \cdot 10^{-5}$	1.000564	$2.2 \cdot 10^{-5}$	0.670868	$2.1 \cdot 10^{-5}$	1.341850	$2.2 \cdot 10^{-5}$
Participant	TB2 - anti-clockwise torque				TT1 - anti-clockwise torque			
	-500 N·m		-1000 N·m		-500 N·m		-1000 N·m	
	$Y_{P-Creep}$	$W_{P-Creep}$	$Y_{P-Creep}$	$W_{P-Creep}$	$Y_{P-Creep}$	$W_{P-Creep}$	$Y_{P-Creep}$	$W_{P-Creep}$
A	-0.500240	$4.1 \cdot 10^{-5}$	-1.000537	$4.1 \cdot 10^{-5}$	-0.670806	$4.1 \cdot 10^{-5}$	-1.341729	$4.1 \cdot 10^{-5}$
B	-0.500241	$2.1 \cdot 10^{-5}$	-1.000526	$2.2 \cdot 10^{-5}$	-0.670910	$2.1 \cdot 10^{-5}$	-1.341906	$2.2 \cdot 10^{-5}$
C	-0.500270	$3.1 \cdot 10^{-5}$	-1.000587	$3.1 \cdot 10^{-5}$	-0.670771	$3.1 \cdot 10^{-5}$	-1.341633	$3.1 \cdot 10^{-5}$
D	-0.500258	$5.1 \cdot 10^{-5}$	-1.000560	$5.0 \cdot 10^{-5}$	-0.670879	$5.1 \cdot 10^{-5}$	-1.341842	$5.0 \cdot 10^{-5}$
E	-0.500246	$1.0 \cdot 10^{-4}$	-1.000540	$1.0 \cdot 10^{-4}$	-0.670805	$1.0 \cdot 10^{-4}$	-1.341689	$1.0 \cdot 10^{-4}$
F	-0.500293	$5.3 \cdot 10^{-5}$	-1.000654	$4.7 \cdot 10^{-5}$	-0.670893	$4.1 \cdot 10^{-5}$	-1.341845	$4.2 \cdot 10^{-5}$
G	-0.500262	$2.2 \cdot 10^{-5}$	-1.000571	$2.3 \cdot 10^{-5}$	-0.670853	$2.3 \cdot 10^{-5}$	-1.341801	$2.4 \cdot 10^{-5}$
H	-0.500249	$2.1 \cdot 10^{-5}$	-1.000531	$2.2 \cdot 10^{-5}$	-0.670851	$2.1 \cdot 10^{-5}$	-1.341787	$2.2 \cdot 10^{-5}$

Table 10: Deflections from table 9 in mV/V, additionally corrected for the influence of the environment, and corresponding expanded relative uncertainties ($k = 2$)

Participant	TB2 - clockwise torque				TT1 - clockwise torque			
	500 N·m		1000 N·m		500 N·m		1000 N·m	
	$Y_{P-Envir}$	$W_{P-Envir}$	$Y_{P-Envir}$	$W_{P-Envir}$	$Y_{P-Envir}$	$W_{P-Envir}$	$Y_{P-Envir}$	$W_{P-Envir}$
A	0.500264	$4.2 \cdot 10^{-5}$	1.000596	$4.1 \cdot 10^{-5}$	0.670873	$5.1 \cdot 10^{-5}$	1.341877	$5.3 \cdot 10^{-5}$
B	0.500253	$2.5 \cdot 10^{-5}$	1.000567	$2.4 \cdot 10^{-5}$	0.670888	$5.0 \cdot 10^{-5}$	1.341893	$5.4 \cdot 10^{-5}$
C	0.500273	$3.5 \cdot 10^{-5}$	1.000614	$3.4 \cdot 10^{-5}$	0.670835	$6.7 \cdot 10^{-5}$	1.341779	$7.3 \cdot 10^{-5}$
D	0.500275	$5.1 \cdot 10^{-5}$	1.000608	$5.0 \cdot 10^{-5}$	0.670887	$5.2 \cdot 10^{-5}$	1.341902	$5.2 \cdot 10^{-5}$
E	0.500249	$1.0 \cdot 10^{-4}$	1.000569	$1.0 \cdot 10^{-4}$	0.670841	$1.1 \cdot 10^{-4}$	1.341789	$1.1 \cdot 10^{-4}$
F	0.500253	$5.6 \cdot 10^{-5}$	1.000601	$4.4 \cdot 10^{-5}$	0.670839	$6.2 \cdot 10^{-5}$	1.341815	$6.4 \cdot 10^{-5}$
G	0.500254	$2.6 \cdot 10^{-5}$	1.000568	$2.3 \cdot 10^{-5}$	0.670851	$4.4 \cdot 10^{-5}$	1.341815	$4.7 \cdot 10^{-5}$
H	0.500254	$2.1 \cdot 10^{-5}$	1.000564	$2.2 \cdot 10^{-5}$	0.670868	$2.3 \cdot 10^{-5}$	1.341850	$2.4 \cdot 10^{-5}$
Participant	TB2 - anti-clockwise torque				TT1 - anti-clockwise torque			
	-500 N·m		-1000 N·m		-500 N·m		-1000 N·m	
	$Y_{P-Envir}$	$W_{P-Envir}$	$Y_{P-Envir}$	$W_{P-Envir}$	$Y_{P-Envir}$	$W_{P-Envir}$	$Y_{P-Envir}$	$W_{P-Envir}$
A	-0.500238	$4.1 \cdot 10^{-5}$	-1.000535	$4.1 \cdot 10^{-5}$	-0.670826	$5.1 \cdot 10^{-5}$	-1.341770	$5.3 \cdot 10^{-5}$
B	-0.500244	$2.6 \cdot 10^{-5}$	-1.000530	$2.5 \cdot 10^{-5}$	-0.670875	$5.6 \cdot 10^{-5}$	-1.341835	$6.2 \cdot 10^{-5}$
C	-0.500266	$3.6 \cdot 10^{-5}$	-1.000583	$3.5 \cdot 10^{-5}$	-0.670809	$6.4 \cdot 10^{-5}$	-1.341709	$6.9 \cdot 10^{-5}$
D	-0.500259	$5.1 \cdot 10^{-5}$	-1.000561	$5.0 \cdot 10^{-5}$	-0.670871	$5.2 \cdot 10^{-5}$	-1.341828	$5.2 \cdot 10^{-5}$
E	-0.500243	$1.0 \cdot 10^{-4}$	-1.000537	$1.0 \cdot 10^{-4}$	-0.670822	$1.0 \cdot 10^{-4}$	-1.341723	$1.1 \cdot 10^{-4}$
F	-0.500292	$5.3 \cdot 10^{-5}$	-1.000653	$4.7 \cdot 10^{-5}$	-0.670908	$4.8 \cdot 10^{-5}$	-1.341875	$4.9 \cdot 10^{-5}$
G	-0.500259	$2.5 \cdot 10^{-5}$	-1.000569	$2.5 \cdot 10^{-5}$	-0.670849	$2.5 \cdot 10^{-5}$	-1.341792	$2.6 \cdot 10^{-5}$
H	-0.500249	$2.1 \cdot 10^{-5}$	-1.000531	$2.2 \cdot 10^{-5}$	-0.670851	$2.3 \cdot 10^{-5}$	-1.341787	$2.4 \cdot 10^{-5}$

The expanded relative uncertainties W_{P-Rep} , W_{P-DMP} , $W_{P-Creep}$ and $W_{P-Envir}$ are calculated using

$$W_{P-Rep} = 2 \cdot w_{P-Rep} = 2 \cdot \sqrt{w_{Repeat}^2 + w_{Reprod}^2 + 2 \cdot w_{Ind}^2 + w_{TSM}^2} \quad (13)$$

$$W_{P-DMP} = 2 \cdot w_{P-DMP} = 2 \cdot \sqrt{w_{P-Rep}^2 + w_{DMP}^2} \quad (14)$$

$$W_{P-Creep} = 2 \cdot w_{P-Creep} = 2 \cdot \sqrt{w_{P-DMP}^2 + w_{Creep}^2} \quad (15)$$

$$W_{P-Envir} = 2 \cdot w_{P-Envir} = 2 \cdot \sqrt{w_{P-Creep}^2 + w_{Envir}^2} \quad (16)$$

with

- the repeatability w_{Repeat} , calculated as relative standard deviation of the mean value of the deflections from three runs 1, 2 and 3,
- the reproducibility w_{Reprod} , calculated as relative standard deviation of the mean value of the deflections from twelve runs 4 to 15,
- the uncertainty contribution of the indication w_{Ind} , calculated as relative standard uncertainty of the indication using a rectangular distribution (the indication is given by the span of the signal change under stable conditions without the torque applied to the transducer and cannot be better than the numerical resolution)
- the uncertainty of the applied torque defined by the participant's torque standard machine (TSM) w_{TSM} ,
- the uncertainty contribution of the correction for DMP40 deviations w_{DMP} , calculated applying the GUM procedure to equation (1)
- the uncertainty contribution of the creep correction w_{Creep} , calculated applying the GUM procedure to equation (2), and
- the uncertainty contribution of the correction for environmental deviations w_{Envir} , calculated applying the GUM procedure to equation (12).

8. Summary

The results of the measurements (deflections and uncertainties) reported by the participants of the CIPM key comparison CCM.T-K1 to the pilot laboratory were evaluated. Some known effects were included into the evaluation by correction terms. In detail, corrections for the deviations of the amplifiers of the participating laboratories, the creep influence due to different loading times in the machines and the environmental conditions on site were calculated.

The Annex contains the calculation of the key comparison reference values, the corresponding uncertainties, the relative deviations of the values from the reference value and the degrees of equivalence.

References

- [1] *D. Röske*, Key comparisons in the field of torque measurement, Presentation and Paper at the 19th International IMEKO TC3 Conference on Force, Mass and Torque, February 19-23, 2005, Cairo/Egypt, on Proceedings-CD file \pdf\36.pdf
- [2] *D. Röske, D. Mauersberger*, On the stability of measuring devices for torque key comparisons, IMEKO XVIII World Congress and IV Brazilian Congress of Metrology, September 17-22, 2006, Rio de Janeiro/Brazil, on Proceedings-CD file \trabalhos\00181.pdf, Internet-Link: <http://www.imeko.org/publications/wc-2006/PWC-2006-TC3-040u.pdf>
- [3] *M. G. Cox*, The Evaluation of key comparison data, *Metrologia*, 2002, **39**, 589-595

ANNEX to: Final Report on the Torque Key Comparison CCM.T-K1

Measurand Torque: 0 N·m, 500 N·m, 1000 N·m

A.1 Weighted means, χ^2 tests and key comparison reference values

The weighted means and their corresponding uncertainties were calculated according to procedure A in [3]. A χ^2 test was performed on the data in order to check the consistency of the corrected values. For the clockwise torque, the results shown in table A11 were obtained.

Table A11: Results of a χ^2 test on the corrected clockwise values from all participants (ν - degree of freedom = number of participants - 1)

	TB2		TT1	
	500 N·m cw	1000 N·m cw	500 N·m cw	1000 N·m cw
χ^2_{obs}	6.77	11.07	8.57	8.87
ν	7	7	7	7
$\chi^2(\nu), P = 0,05$	14.07	14.07	14.07	14.07
Result	Test passed	Test passed	Test passed	Test passed

For all clockwise measurements the values passed the χ^2 test, therefore the corrected values were considered to be consistent and the weighted means were taken as the key comparison reference values for clockwise torque.

For the anti-clockwise torque, the results shown in table A12 were obtained.

Table A12: Results of a χ^2 test on the corrected anti-clockwise values from all participants (ν - degree of freedom = number of participants - 1)

	TB2		TT1	
	500 N·m acw	1000 N·m acw	500 N·m acw	1000 N·m acw
χ^2_{obs}	16.61	31.71	22.18	12.82
ν	7	7	7	7
$\chi^2(\nu), P = 0,05$	14.07	14.07	14.07	14.07
Result	Test failed	Test failed	Test failed	Test passed

Three out of four anti-clockwise measurements did not pass the χ^2 test. The reason was that the corrected values of one of the participants (F) deviated from the mean value by an up to two times higher amount compared with the corresponding uncertainty due to temperature influences during the measurements and resulting problems. Therefore, the anti-clockwise results of participant F were considered to be an outlier and it is recommended to exclude this participant from the evaluation of the anti-clockwise direction. The tests were repeated with the reduced number of participants and the results shown in table A13 were obtained.

Table A13: Results of a χ^2 test on the corrected anti-clockwise values from all participants, except participant F (ν - degree of freedom = number of participants - 1)

	TB2		TT1	
	500 N·m acw	1000 N·m acw	500 N·m acw	1000 N·m acw
χ^2_{obs}	7.61	12.34	9.62	6.61
ν	6	6	6	6
$\chi^2(\nu), P = 0,05$	12.59	12.59	12.59	12.59
Result	Test passed	Test passed	Test passed	Test passed

Now all anti-clockwise measurements passed the χ^2 test and the corrected values of all participants, except participant F were considered to be consistent and the weighted means were taken as the key comparison reference values for anti-clockwise torque. All calculated "mV/V" key comparison reference values ($KCRV_{mV/V}$) x'_{ref} and their corresponding uncertainties $u(x'_{\text{ref}})$ are given in table A14.

Table A14: Key comparison reference values x'_{ref} in mV/V and corresponding standard uncertainties $u(x'_{\text{ref}})$

	TB2 cw		TB2 acw		TT1 cw		TT1 acw	
	x'_{ref} in mV/V	$u(x'_{\text{ref}})$ in nV/V	x'_{ref} in mV/V	$u(x'_{\text{ref}})$ in nV/V	x'_{ref} in mV/V	$u(x'_{\text{ref}})$ in nV/V	x'_{ref} in mV/V	$u(x'_{\text{ref}})$ in nV/V
500 N·m	0.500258	2.9	-0.500252	3.0	0.670866	5.2	-0.670849	4.8
1000 N·m	1.000578	5.5	-1.000547	5.8	1.341850	10.9	-1.341788	10.0

A.2 Relative deviations of the results from the key comparison reference values

For reporting the results and calculating the degrees of equivalence, instead of using the transducer-dependent sensitivities in mV/V from table A14 the round torque values in N·m were taken as the KCRVs x_{ref} . The assigned uncertainties $u(x_{\text{ref}})$ were calculated from the relation

$$u(x_{\text{ref}}) = \frac{x_{\text{ref}}}{x'_{\text{ref}}} \cdot u(x'_{\text{ref}}) \quad (17)$$

and are given in mN·m in table A15.

Table A15: Key comparison reference values x_{ref} in mV/V and corresponding standard uncertainties $u(x_{\text{ref}})$

	TB2 cw		TB2 acw		TT1 cw		TT1 acw	
	x_{ref} in N·m	$u(x_{\text{ref}})$ in mN·m	x_{ref} in N·m	$u(x_{\text{ref}})$ in mN·m	x_{ref} in N·m	$u(x_{\text{ref}})$ in mN·m	x_{ref} in N·m	$u(x_{\text{ref}})$ in mN·m
500 N·m	500.000	2.9	-500.000	3.0	500.000	3.9	-500.000	3.6
1000 N·m	1000.000	5.5	-1000.000	5.8	1000.000	8.1	-1000.000	7.5

The corrected results of the participants given in table 10 in mV/V are now converted to torque units in N·m using

$$Y_{\text{P-N·m}} = \frac{x_{\text{ref}}}{x'_{\text{ref}}} \cdot Y_{\text{P-Envir}} \quad (18)$$

and are given in table A16. The relative uncertainties W don't need to be converted.

Table A16: Deflections from table 10 converted to torque units in N·m and corresponding expanded relative uncertainties ($k = 2$), * participant's result not used for the calculation of the KCRV

Participant	TB2 - clockwise torque				TT1 - clockwise torque			
	500 N·m		1000 N·m		500 N·m		1000 N·m	
	$Y_{\text{P-N·m}}$	$W_{\text{P-N·m}}$	$Y_{\text{P-N·m}}$	$W_{\text{P-N·m}}$	$Y_{\text{P-N·m}}$	$W_{\text{P-N·m}}$	$Y_{\text{P-N·m}}$	$W_{\text{P-N·m}}$
A	500.006	$4.2 \cdot 10^{-5}$	1000.018	$4.1 \cdot 10^{-5}$	500.006	$5.1 \cdot 10^{-5}$	1000.020	$5.3 \cdot 10^{-5}$
B	499.996	$2.5 \cdot 10^{-5}$	999.989	$2.4 \cdot 10^{-5}$	500.017	$5.0 \cdot 10^{-5}$	1000.032	$5.4 \cdot 10^{-5}$
C	500.015	$3.5 \cdot 10^{-5}$	1000.036	$3.4 \cdot 10^{-5}$	499.977	$6.7 \cdot 10^{-5}$	999.947	$7.3 \cdot 10^{-5}$
D	500.017	$5.1 \cdot 10^{-5}$	1000.030	$5.0 \cdot 10^{-5}$	500.016	$5.2 \cdot 10^{-5}$	1000.039	$5.2 \cdot 10^{-5}$
E	499.991	$1.0 \cdot 10^{-4}$	999.991	$1.0 \cdot 10^{-4}$	499.981	$1.1 \cdot 10^{-4}$	999.954	$1.1 \cdot 10^{-4}$
F	499.995	$5.6 \cdot 10^{-5}$	1000.023	$4.4 \cdot 10^{-5}$	499.980	$6.2 \cdot 10^{-5}$	999.974	$6.4 \cdot 10^{-5}$
G	499.997	$2.6 \cdot 10^{-5}$	999.991	$2.3 \cdot 10^{-5}$	499.989	$4.4 \cdot 10^{-5}$	999.974	$4.7 \cdot 10^{-5}$
H	499.996	$2.1 \cdot 10^{-5}$	999.986	$2.2 \cdot 10^{-5}$	500.001	$2.3 \cdot 10^{-5}$	1000.000	$2.4 \cdot 10^{-5}$
Participant	TB2 - anti-clockwise torque				TT1 - anti-clockwise torque			
	-500 N·m		-1000 N·m		-500 N·m		-1000 N·m	
	$Y_{\text{P-N·m}}$	$W_{\text{P-N·m}}$	$Y_{\text{P-N·m}}$	$W_{\text{P-N·m}}$	$Y_{\text{P-N·m}}$	$W_{\text{P-N·m}}$	$Y_{\text{P-N·m}}$	$W_{\text{P-N·m}}$
A	-499.986	$4.1 \cdot 10^{-5}$	-999.987	$4.1 \cdot 10^{-5}$	-499.983	$5.1 \cdot 10^{-5}$	-999.986	$5.3 \cdot 10^{-5}$
B	-499.992	$2.6 \cdot 10^{-5}$	-999.983	$2.5 \cdot 10^{-5}$	-500.020	$5.6 \cdot 10^{-5}$	-1000.035	$6.2 \cdot 10^{-5}$
C	-500.014	$3.6 \cdot 10^{-5}$	-1000.036	$3.5 \cdot 10^{-5}$	-499.970	$6.4 \cdot 10^{-5}$	-999.941	$6.9 \cdot 10^{-5}$
D	-500.007	$5.1 \cdot 10^{-5}$	-1000.013	$5.0 \cdot 10^{-5}$	-500.017	$5.2 \cdot 10^{-5}$	-1000.029	$5.2 \cdot 10^{-5}$
E	-499.992	$1.0 \cdot 10^{-4}$	-999.990	$1.0 \cdot 10^{-4}$	-499.980	$1.0 \cdot 10^{-4}$	-999.952	$1.1 \cdot 10^{-4}$
F *	-500.041	$5.3 \cdot 10^{-5}$	-1000.106	$4.7 \cdot 10^{-5}$	-500.044	$4.8 \cdot 10^{-5}$	-1000.064	$4.9 \cdot 10^{-5}$
G	-500.008	$2.5 \cdot 10^{-5}$	-1000.022	$2.5 \cdot 10^{-5}$	-500.000	$2.5 \cdot 10^{-5}$	-1000.003	$2.6 \cdot 10^{-5}$
H	-499.998	$2.1 \cdot 10^{-5}$	-999.984	$2.2 \cdot 10^{-5}$	-500.002	$2.3 \cdot 10^{-5}$	-999.999	$2.4 \cdot 10^{-5}$

The figures A27 to A34 show the resulting deviations from these KCRVs and their uncertainties.

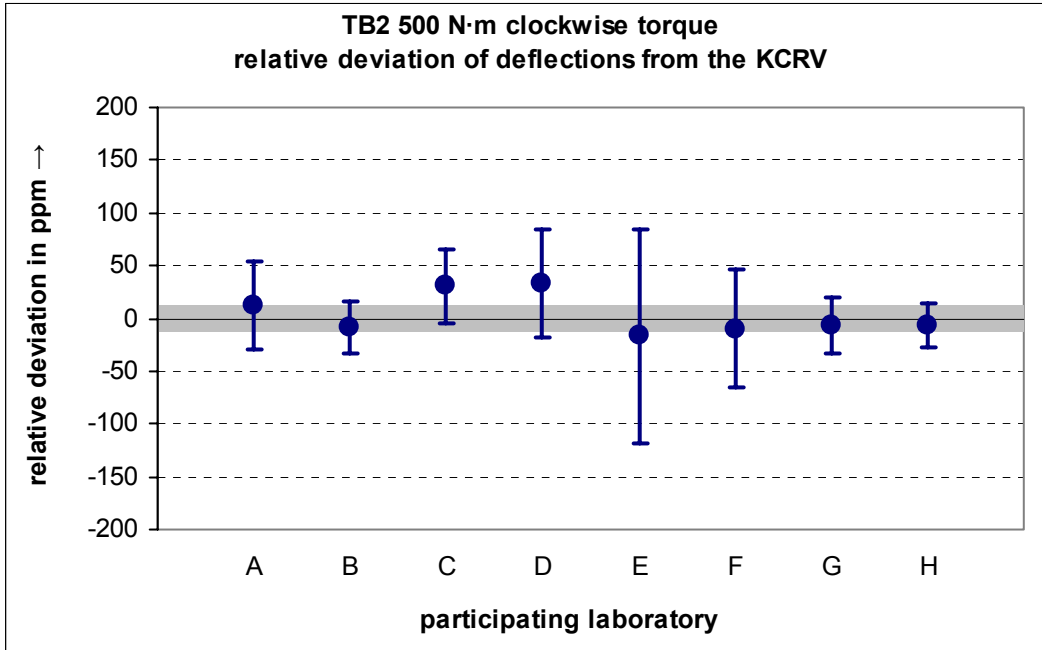


Figure A27. Relative deviations of the corrected deflections for the participating laboratories from the KCRV (grey band = relative expanded uncertainty, $k = 2$) for transducer TB2 at 500 N·m clockwise torque and relative expanded ($k = 2$) measurement uncertainties (uncertainty bars)

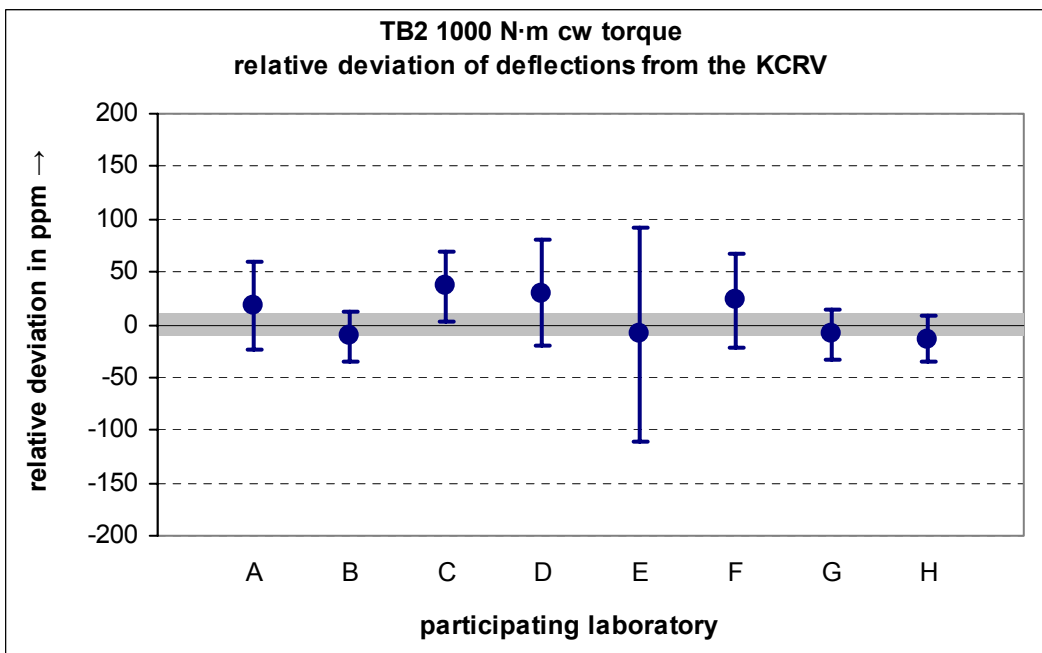


Figure A28. Relative deviations of the corrected deflections for the participating laboratories from the KCRV (grey band = relative expanded uncertainty, $k = 2$) for transducer TB2 at 1000 N·m clockwise torque and relative expanded ($k = 2$) measurement uncertainties (uncertainty bars)

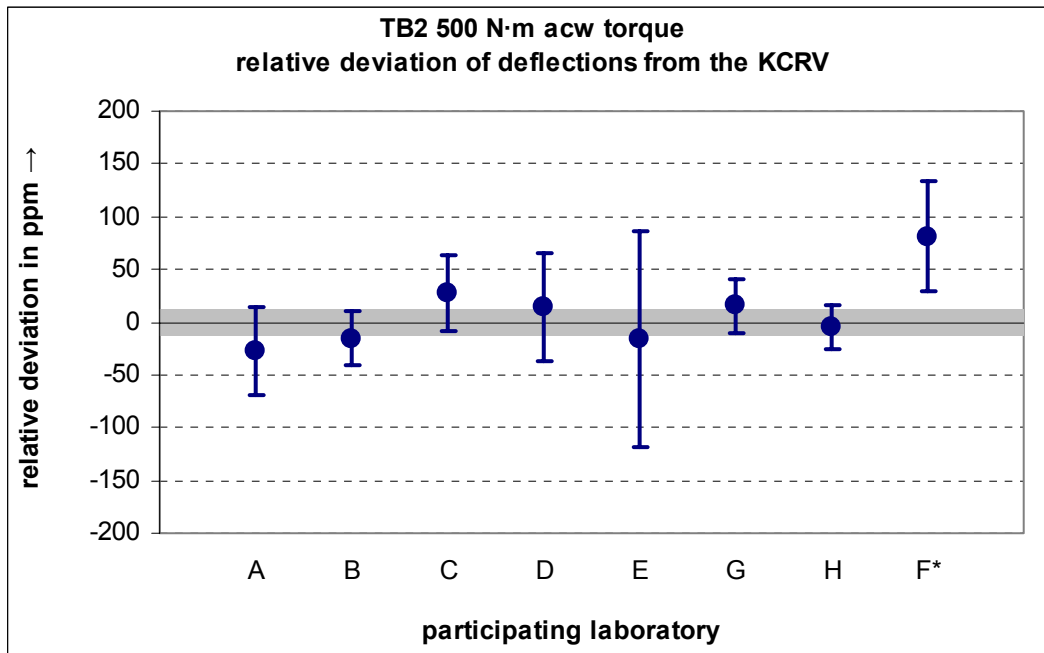


Figure A29. Relative deviations of the corrected deflections for the participating laboratories from the KCRV (* grey band = relative expanded uncertainty, $k = 2$, calculated without F) for transducer TB2 at 500 N·m anti-clockwise torque and relative expanded ($k = 2$) measurement uncertainties (uncertainty bars)

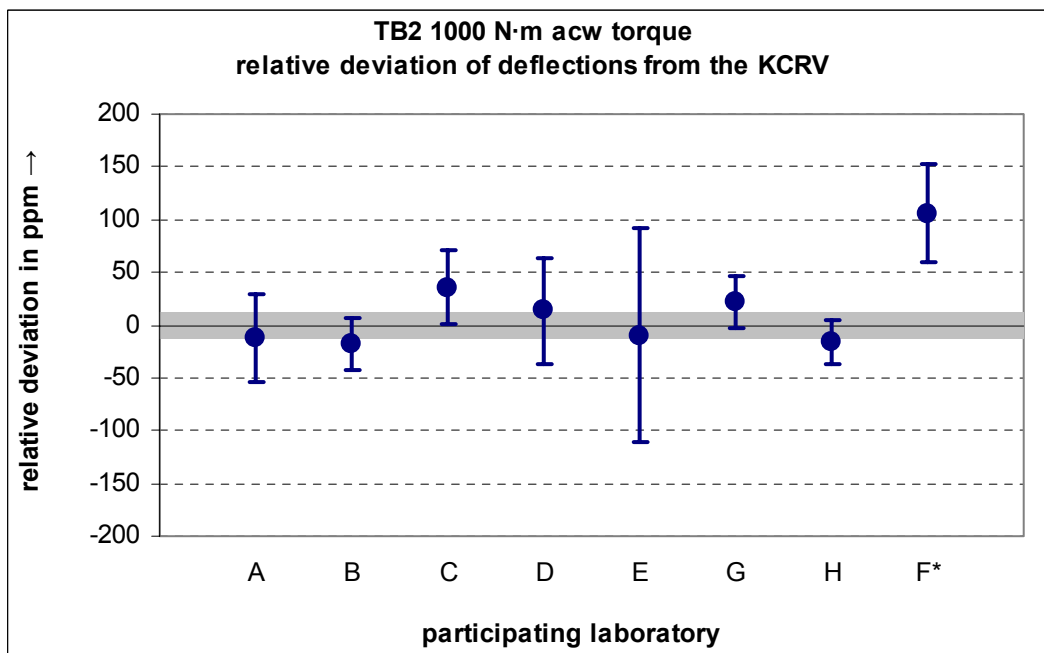


Figure A30. Relative deviations of the corrected deflections for the participating laboratories from the KCRV (* grey band = relative expanded uncertainty, $k = 2$, calculated without F) for transducer TB2 at 1000 N·m anti-clockwise torque and relative expanded ($k = 2$) measurement uncertainties (uncertainty bars)

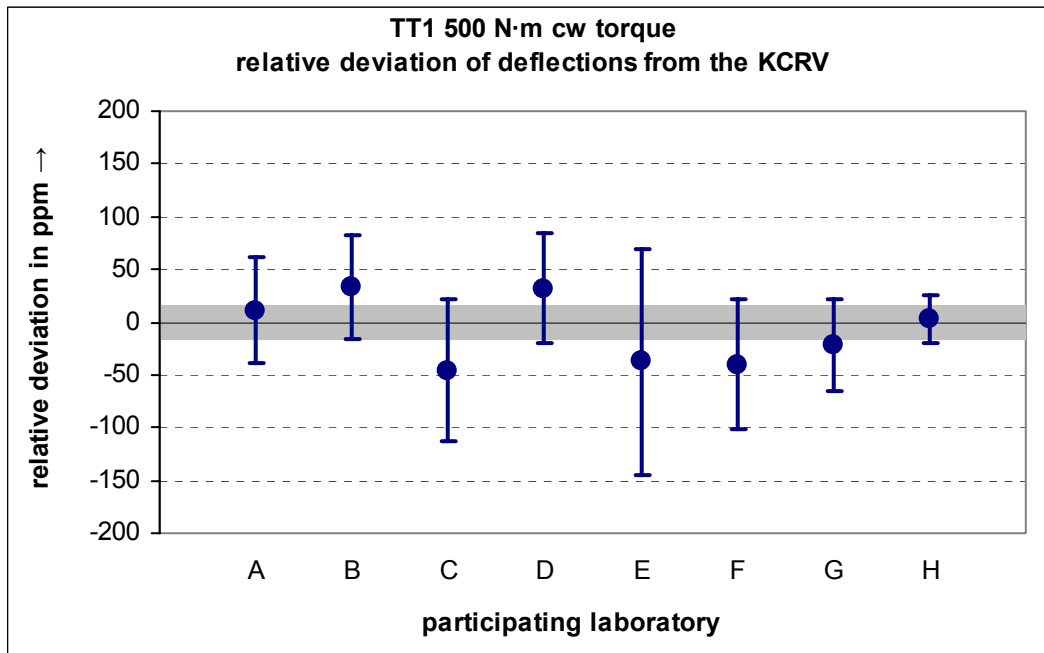


Figure A31. Relative deviations of the corrected deflections for the participating laboratories from the KCRV (grey band = relative expanded uncertainty, $k = 2$) for transducer TT1 at 500 N·m clockwise torque and relative expanded ($k = 2$) measurement uncertainties (uncertainty bars)

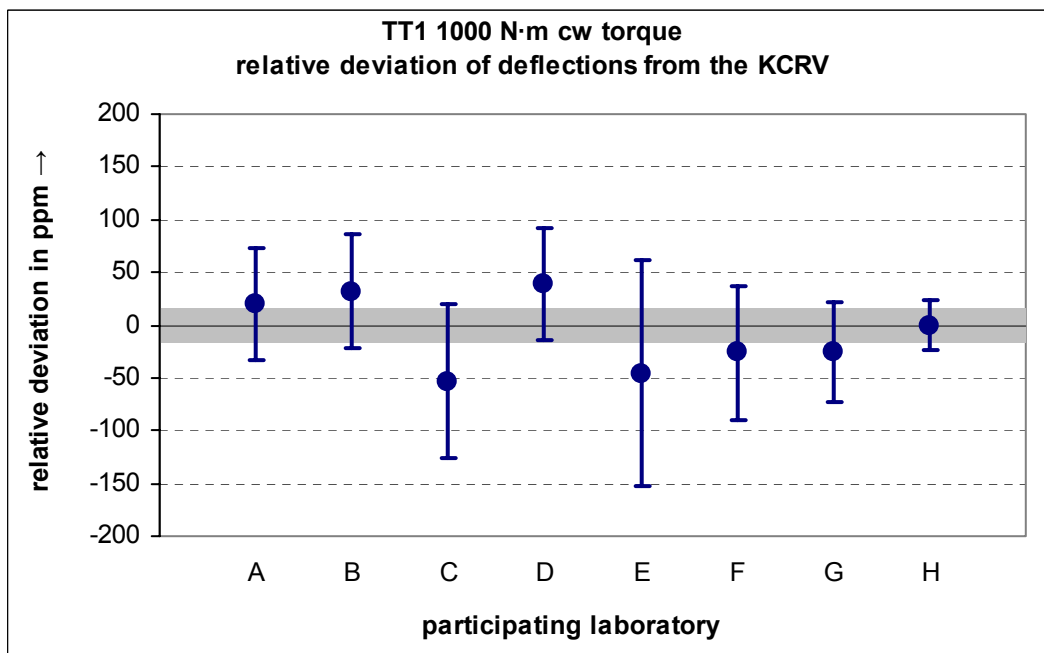


Figure A32. Relative deviations of the corrected deflections for the participating laboratories from the KCRV (grey band = relative expanded uncertainty, $k = 2$) for transducer TT1 at 1000 N·m clockwise torque and relative expanded ($k = 2$) measurement uncertainties (uncertainty bars)

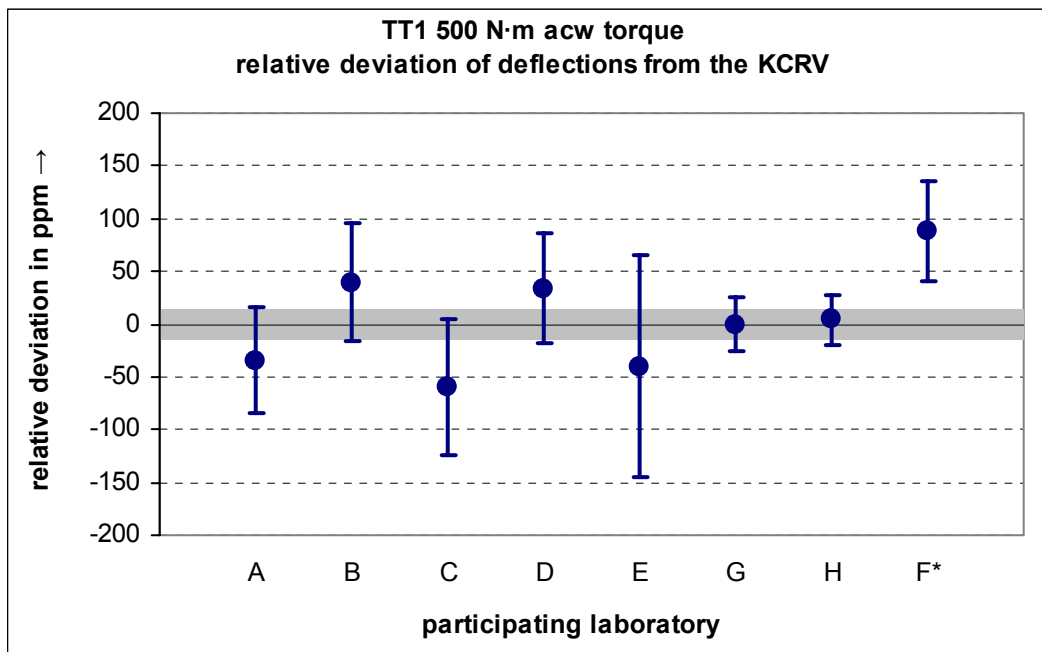


Figure A33. Relative deviations of the corrected deflections for the participating laboratories from the KCRV (* grey band = relative expanded uncertainty, $k = 2$, calculated without F) for transducer TT1 at 500 N·m anti-clockwise torque and relative expanded ($k = 2$) measurement uncertainties (uncertainty bars)

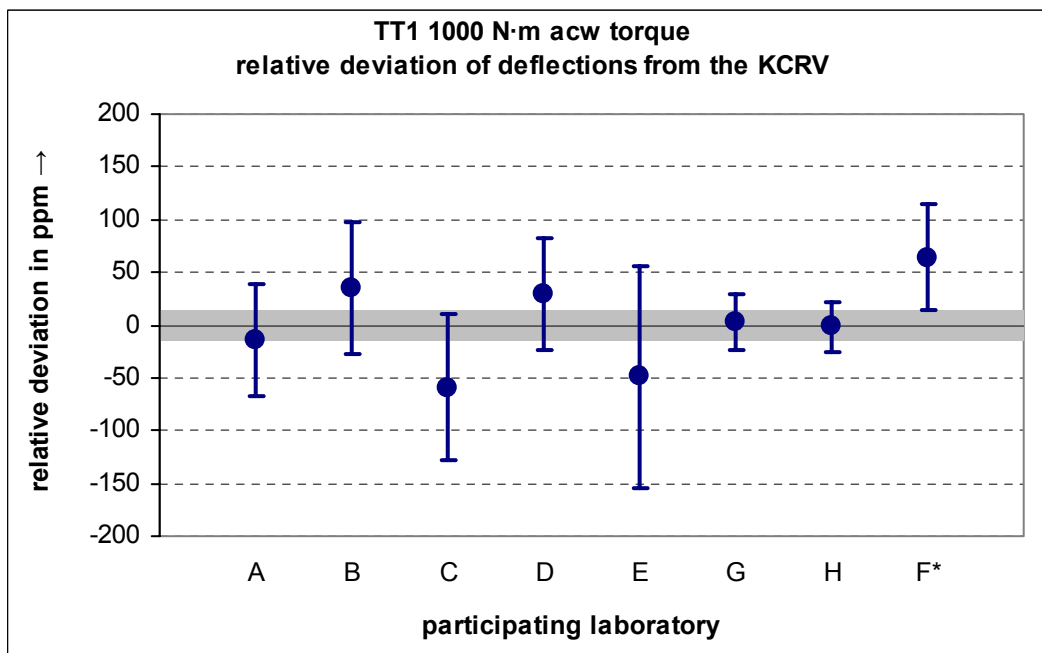


Figure A34. Relative deviations of the corrected deflections for the participating laboratories from the KCRV (* grey band = relative expanded uncertainty, $k = 2$, calculated without F) for transducer TT1 at 1000 N·m anti-clockwise torque and relative expanded ($k = 2$) measurement uncertainties (uncertainty bars)

A.3 Degrees of equivalence

The degrees of equivalence (D_i , $U(D_i)$) between the corrected values from the participants and the key comparison reference values were calculated according to procedure A in [3]. The figures A35 to A42 show the results, the values are given in table A17.

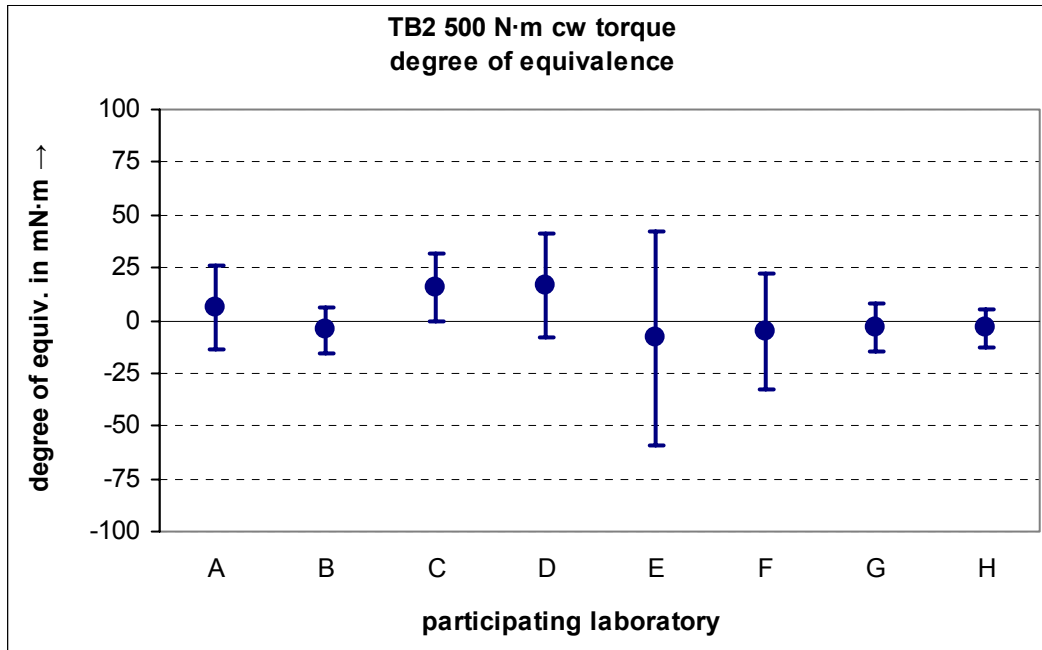


Figure A35. Degrees of equivalence for all measurements made by the participating laboratories with transducer TB2 at 500 N·m clockwise torque (dot = D_i , uncertainty bar = $U(D_i) = U_i$)

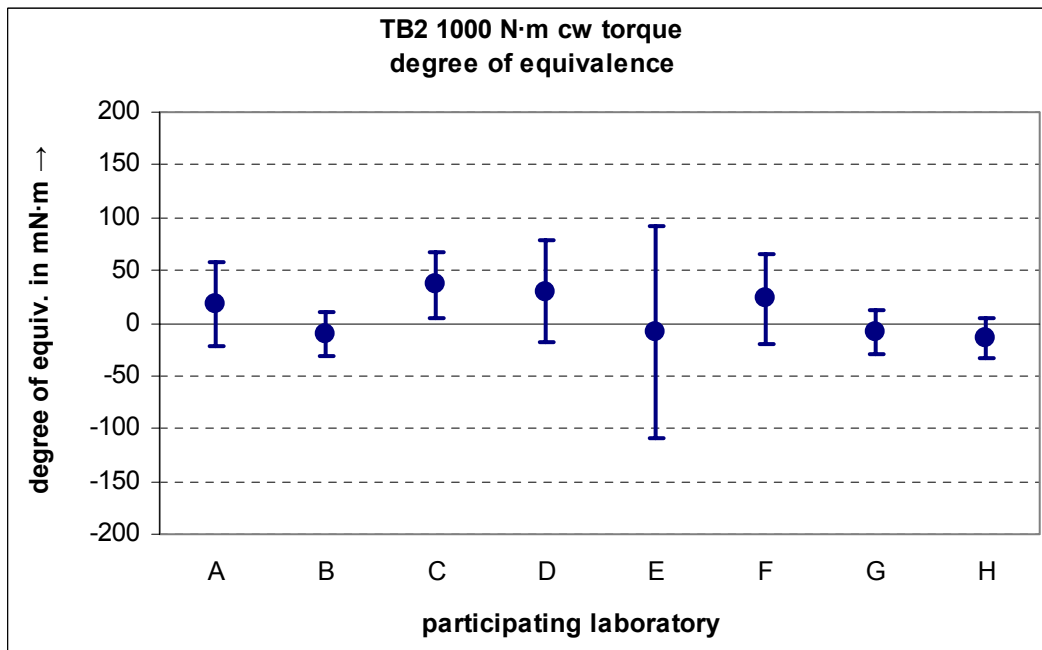


Figure A36. Degrees of equivalence for all measurements made by the participating laboratories with transducer TB2 at 1000 N·m clockwise torque (dot = D_i , uncertainty bar = $U(D_i) = U_i$)

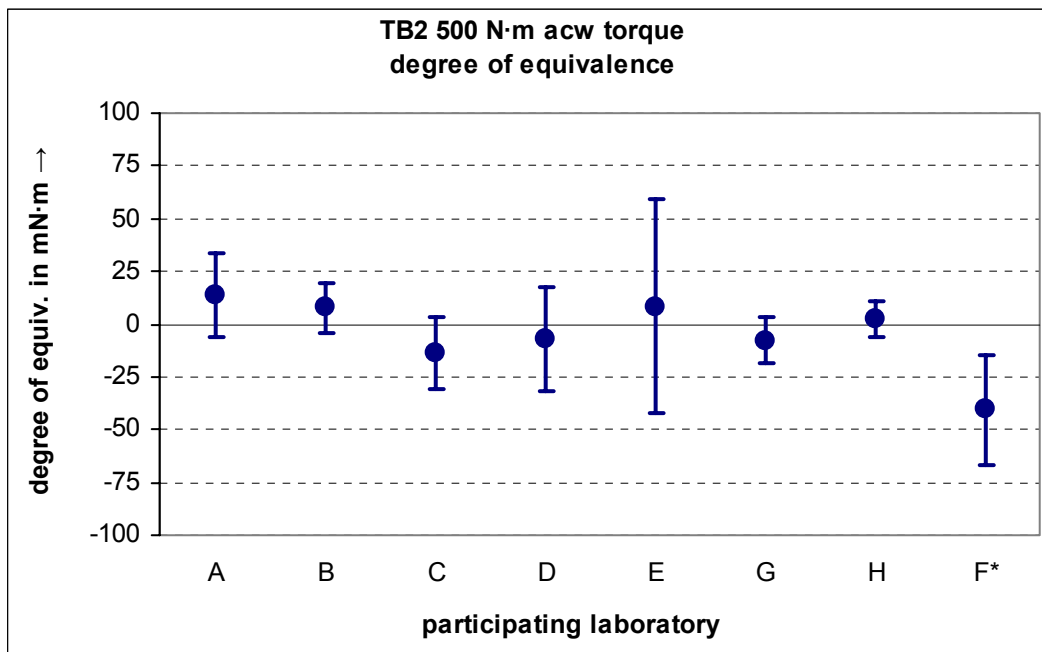


Figure A37. Degrees of equivalence for all measurements made by the participating laboratories with transducer TB2 at 500 N·m anti-clockwise torque (dot = D_i , uncertainty bar = $U(D_i) = U_i$), * KCRV calculated without F

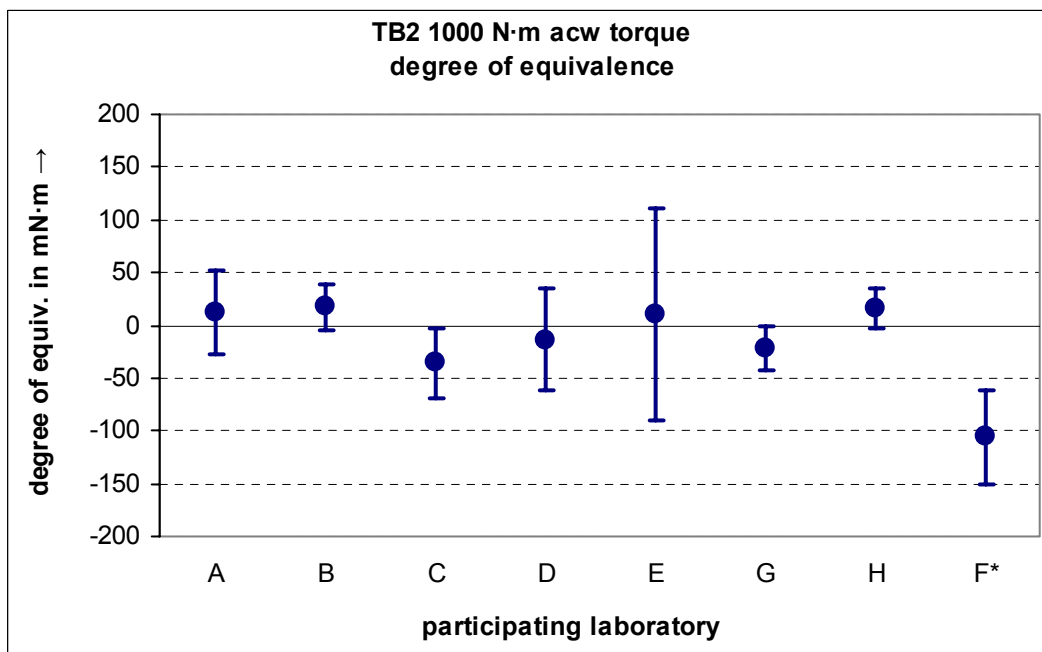


Figure A38. Degrees of equivalence for all measurements made by the participating laboratories with transducer TB2 at 1000 N·m anti-clockwise torque (dot = D_i , uncertainty bar = $U(D_i) = U_i$), * KCRV calculated without F

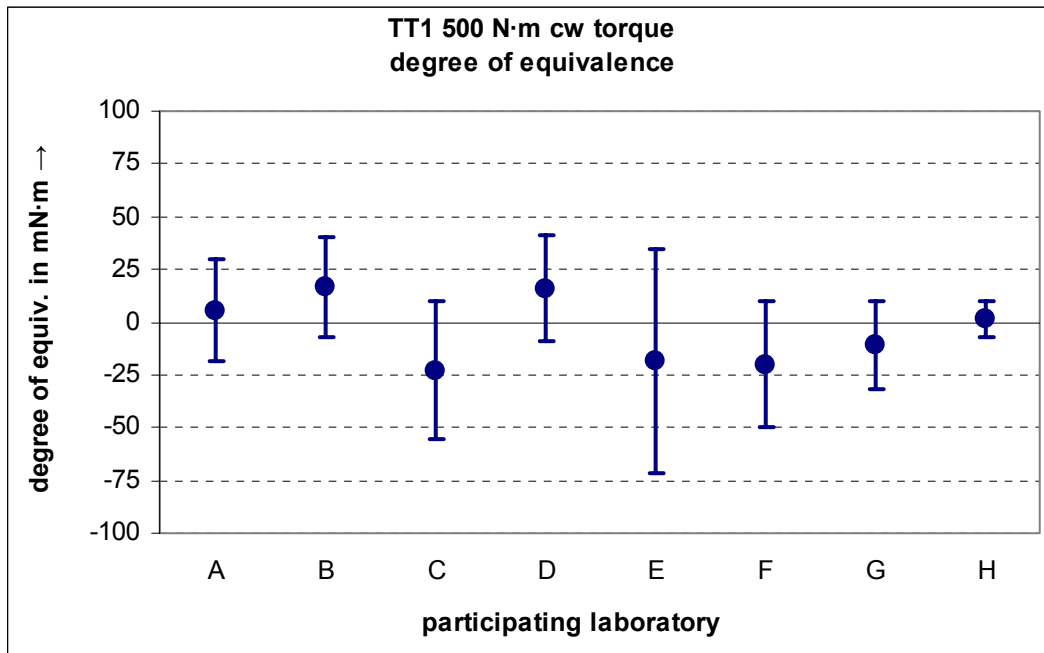


Figure A39. Degrees of equivalence for all measurements made by the participating laboratories with transducer TT1 at 500 N·m clockwise torque (dot = D_i , uncertainty bar = $U(D_i) = U_i$)

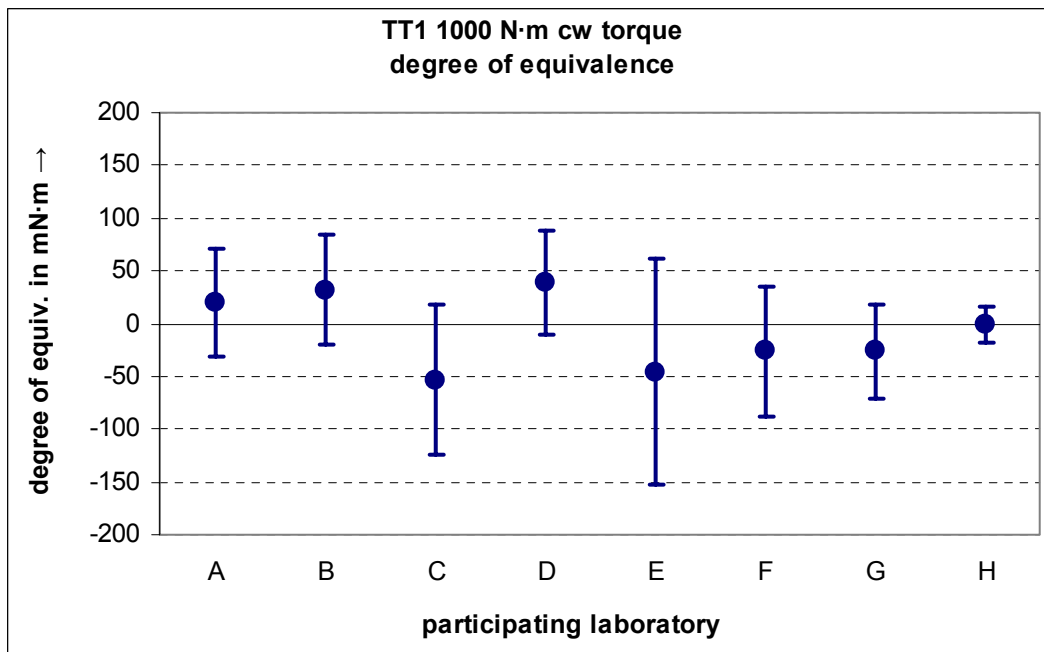


Figure A40. Degrees of equivalence for all measurements made by the participating laboratories with transducer TT1 at 1000 N·m clockwise torque (dot = D_i , uncertainty bar = $U(D_i) = U_i$)

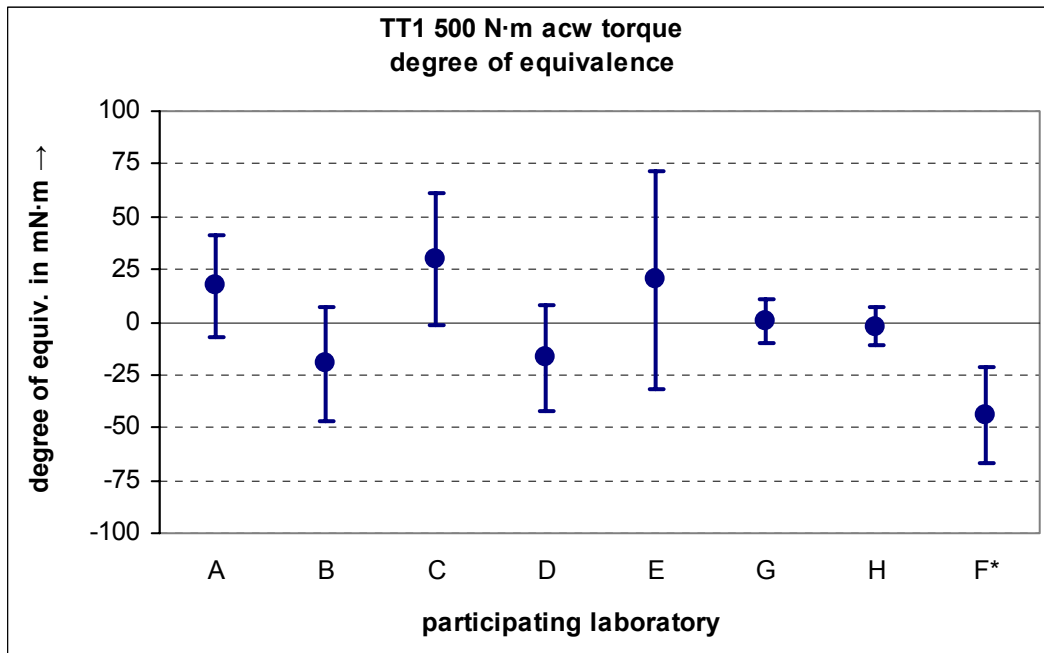


Figure A41. Degrees of equivalence for all measurements made by the participating laboratories with transducer TT1 at 500 N·m anti-clockwise torque (dot = D_i , uncertainty bar = $U(D_i) = U_i$), * KCRV calculated without F

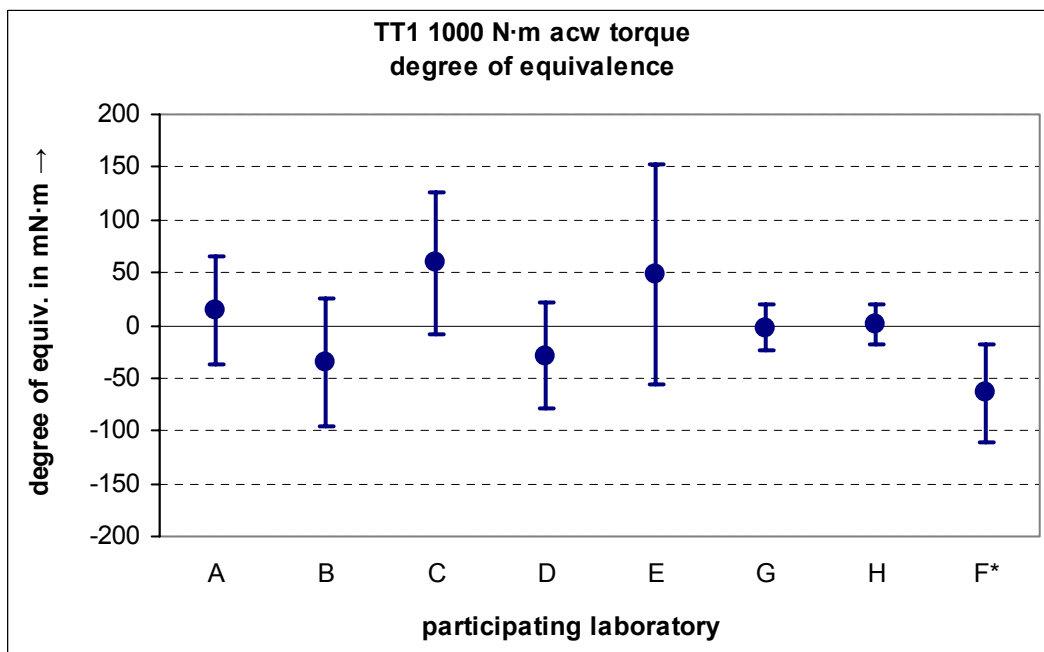


Figure A42. Degrees of equivalence for all measurements made by the participating laboratories with transducer TT1 at 1000 N·m anti-clockwise torque (dot = D_i , uncertainty bar = $U(D_i) = U_i$), * KCRV calculated without F

Table A18 shows the degrees of equivalence (D_{ij} , $U(D_{ij})$) between the corrected values from the participants considering the last as pairs (i, j) for each of the transducers and both steps. The value in a cell was calculated as the difference between the result of the participant in the corresponding row and the result of the participant in the corresponding column. For example, the value -10.6 mN·m in the second column is the difference result(B) – result(A), 10.6 mN·m in the second row is the difference result(A) – result(B), respectively.

Table A17: Degrees of equivalence ($D_i, U(D_i)$) in mN·m between the corrected values from the participants and the corresponding key comparison reference value (* anti-clockwise result not used for the calculation of the KCRV)

$(d_i, U(d_i))$ in mN·m	TB2 cw		TB2 acw	
	500 N·m	1000 N·m	500 N·m	1000 N·m
A	(6.2; 20.0)	(18.0; 39.9)	(13.8; 19.9)	(12.6; 39.7)
B	(-4.4; 10.9)	(-10.6; 21.0)	(7.6; 11.5)	(17.4; 21.7)
C	(15.5; 16.4)	(36.3; 31.7)	(-13.9; 17.1)	(-35.8; 32.6)
D	(16.8; 24.7)	(30.3; 49.1)	(-7.2; 24.7)	(-13.3; 49.0)
E	(-8.5; 50.7)	(-9.1; 100.6)	(8.3; 50.8)	(10.0; 100.5)
F *	(-4.9; 27.5)	(23.1; 43.1)	(-40.7; 25.8)	(-105.9; 45.2)
G	(-3.4; 11.7)	(-9.2; 20.7)	(-7.7; 11.2)	(-21.8; 21.6)
H	(-3.7; 8.8)	(-14.0; 18.7)	(2.3; 8.7)	(16.1; 18.3)
$(d_i, U(d_i))$ in mN·m	TT1 cw		TT1 acw	
	500 N·m	1000 N·m	500 N·m	1000 N·m
A	(5.7; 24.2)	(19.7; 50.5)	(17.1; 24.4)	(14.0; 50.9)
B	(16.8; 23.6)	(32.2; 52.0)	(-19.8; 27.3)	(-34.9; 60.2)
C	(-23.0; 32.7)	(-53.4; 71.3)	(29.9; 31.1)	(59.2; 67.8)
D	(16.1; 25.0)	(39.0; 49.8)	(-16.8; 25.2)	(-29.3; 50.2)
E	(-18.6; 52.9)	(-45.5; 106.4)	(19.9; 52.0)	(48.5; 104.0)
F *	(-20.0; 30.1)	(-25.9; 61.7)	(-44.0; 22.7)	(-64.4; 47.2)
G	(-10.9; 20.7)	(-26.0; 44.6)	(0.2; 10.5)	(-2.7; 21.7)
H	(1.3; 8.4)	(-0.2; 17.2)	(-1.9; 8.9)	(1.2; 18.4)

Table A18: Degrees of equivalence ($D_{ij}, U(D_{ij})$) in mN·m between the corrected values from the participants (* anti-clockwise result not used for the KCRV calculation) – to be continued on the next page

	A		B		C		D	
A	TB2, 500 N·m	TB2, -500 N·m	(10.6; 24.2)	(6.2; 24.4)	(-9.3; 27.1)	(27.7; 27.5)	(-10.5; 32.8)	(20.9; 32.8)
	TB2, 1000 N·m	TB2, -1000 N·m	(28.5; 47.7)	(-4.8; 48.2)	(-18.4; 53.3)	(48.4; 54.0)	(-12.3; 65.2)	(25.9; 65.2)
	TT1, 500 N·m	TT1, -500 N·m	(-11.2; 35.5)	(37.0; 38.0)	(28.7; 42.1)	(-12.7; 40.8)	(-10.4; 36.5)	(33.9; 36.5)
	TT1, 1000 N·m	TT1, -1000 N·m	(-12.4; 76.0)	(48.9; 81.6)	(73.1; 90.3)	(-45.2; 87.4)	(-19.2; 74.5)	(43.3; 74.5)
B	(-10.6; 24.2)	(-6.2; 24.4)	TB2, 500 N·m	TB2, -500 N·m	(-19.9; 21.3)	(21.6; 22.3)	(-21.1; 28.2)	(14.8; 28.5)
	(-28.5; 47.7)	(4.8; 48.2)	TB2, 1000 N·m	TB2, -1000 N·m	(-46.9; 41.1)	(53.2; 42.4)	(-40.9; 55.6)	(30.7; 56.0)
	(11.2; 35.5)	(-37.0; 38.0)	TT1, 500 N·m	TT1, -500 N·m	(39.8; 41.7)	(-49.7; 42.6)	(0.8; 36.1)	(-3.0; 38.5)
	(12.4; 76.0)	(-48.9; 81.6)	TT1, 1000 N·m	TT1, -1000 N·m	(85.6; 91.2)	(-94.1; 93.1)	(-6.8; 75.5)	(-5.6; 81.2)
C	(9.3; 27.1)	(-27.7; 27.5)	(19.9; 21.3)	(-21.6; 22.3)	TB2, 500 N·m	TB2, -500 N·m	(-1.3; 30.8)	(-6.8; 31.2)
	(18.4; 53.3)	(-48.4; 54.0)	(46.9; 41.1)	(-53.2; 42.4)	TB2, 1000 N·m	TB2, -1000 N·m	(6.0; 60.5)	(-22.5; 61.1)
	(-28.7; 42.1)	(12.7; 40.8)	(-39.8; 41.7)	(49.7; 42.6)	TT1, 500 N·m	TT1, -500 N·m	(-39.1; 42.6)	(46.7; 41.3)
	(-73.1; 90.3)	(45.2; 87.4)	(-85.6; 91.2)	(94.1; 93.1)	TT1, 1000 N·m	TT1, -1000 N·m	(-92.3; 90.0)	(88.5; 87.0)
D	(10.5; 32.8)	(-20.9; 32.8)	(21.1; 28.2)	(-14.8; 28.5)	(1.3; 30.8)	(6.8; 31.2)	TB2, 500 N·m	TB2, -500 N·m
	(12.3; 65.2)	(-25.9; 65.2)	(40.9; 55.6)	(-30.7; 56.0)	(-6.0; 60.5)	(22.5; 61.1)	TB2, 1000 N·m	TB2, -1000 N·m
	(10.4; 36.5)	(-33.9; 36.5)	(-0.8; 36.1)	(3.0; 38.5)	(39.1; 42.6)	(-46.7; 41.3)	TT1, 500 N·m	TT1, -500 N·m
	(19.2; 74.5)	(-43.3; 74.5)	(6.8; 75.5)	(5.6; 81.2)	(92.3; 90.0)	(-88.5; 87.0)	TT1, 1000 N·m	TT1, -1000 N·m
E	(-14.7; 55.1)	(-5.5; 55.1)	(-4.1; 52.5)	(0.7; 52.7)	(-24.0; 53.9)	(22.2; 54.2)	(-25.3; 57.0)	(15.4; 57.1)
	(-27.0; 109.3)	(-2.6; 109.4)	(1.5; 103.9)	(-7.4; 104.1)	(-45.4; 106.6)	(45.8; 107.0)	(-39.4; 113.0)	(23.3; 113.0)
	(-24.3; 59.2)	(2.8; 58.3)	(-35.5; 59.0)	(39.7; 59.6)	(4.4; 63.2)	(-10.0; 61.4)	(-34.7; 59.6)	(36.7; 58.7)
	(-65.3; 120.0)	(34.5; 117.7)	(-77.7; 120.6)	(83.4; 122.0)	(7.8; 130.1)	(-10.7; 126.0)	(-84.5; 119.7)	(77.8; 117.4)
F *	(-11.1; 34.9)	(-54.5; 33.6)	(-0.5; 30.6)	(-48.3; 29.4)	(-20.3; 33.0)	(-26.7; 32.1)	(-21.6; 37.8)	(-33.5; 36.7)
	(5.1; 60.7)	(-118.6; 62.4)	(33.7; 50.4)	(-123.3; 52.8)	(-13.3; 55.7)	(-70.2; 58.1)	(-7.2; 67.1)	(-92.6; 68.7)
	(-25.6; 40.2)	(-61.1; 34.8)	(-36.8; 39.8)	(-24.2; 36.9)	(3.0; 45.8)	(-73.8; 39.8)	(-36.0; 40.7)	(-27.2; 35.4)
	(-45.6; 82.9)	(-78.4; 72.5)	(-58.1; 83.8)	(-29.5; 79.3)	(27.5; 97.1)	(-123.5; 85.3)	(-64.8; 82.5)	(-35.1; 72.0)
G	(-9.6; 24.6)	(-21.4; 24.3)	(1.0; 17.9)	(-15.3; 18.1)	(-18.9; 21.7)	(6.3; 22.1)	(-20.2; 28.6)	(-0.5; 28.4)
	(-27.2; 47.6)	(-34.5; 48.2)	(1.4; 33.3)	(-39.2; 34.8)	(-45.5; 41.0)	(13.9; 42.4)	(-39.5; 55.5)	(-8.5; 56.0)
	(-16.6; 33.7)	(-17.0; 28.4)	(-27.7; 33.3)	(20.0; 31.0)	(12.1; 40.2)	(-29.7; 34.4)	(-27.0; 34.3)	(17.0; 29.1)
	(-45.7; 71.1)	(-16.7; 59.2)	(-58.2; 72.2)	(32.2; 67.4)	(27.4; 87.2)	(-61.9; 74.3)	(-64.9; 70.6)	(26.6; 58.6)
H	(-9.9; 23.3)	(-11.5; 23.2)	(0.7; 16.2)	(-5.3; 16.7)	(-19.2; 20.3)	(16.2; 21.0)	(-20.4; 27.5)	(9.4; 27.5)
	(-31.9; 46.7)	(3.5; 46.8)	(-3.4; 32.1)	(-1.3; 32.8)	(-50.3; 40.0)	(51.9; 40.8)	(-44.3; 54.8)	(29.4; 54.8)
	(-4.4; 27.8)	(-19.1; 27.8)	(-15.5; 27.3)	(17.9; 30.5)	(24.3; 35.5)	(-31.8; 33.9)	(-14.7; 28.6)	(14.9; 28.6)
	(-19.9; 58.0)	(-12.8; 58.1)	(-32.4; 59.3)	(36.1; 66.4)	(53.2; 76.9)	(-58.0; 73.4)	(-39.1; 57.4)	(30.5; 57.5)

Table A18 - continued: Degrees of equivalence (D_{ij} , $U(D_{ij})$) in mN·m between the corrected values from the participants (* anti-clockwise result not used for the KCRV calculation)

	E		F *		G		H	
A	(14.7; 55.1)	(5.5; 55.1)	(11.1; 34.9)	(54.5; 33.6)	(9.6; 24.6)	(21.4; 24.3)	(9.9; 23.3)	(11.5; 23.2)
	(27.0; 109.3)	(2.6; 109.4)	(-5.1; 60.7)	(118.6; 62.4)	(27.2; 47.6)	(34.5; 48.2)	(31.9; 46.7)	(-3.5; 46.8)
	(24.3; 59.2)	(-2.8; 58.3)	(25.6; 40.2)	(61.1; 34.8)	(16.6; 33.7)	(17.0; 28.4)	(4.4; 27.8)	(19.1; 27.8)
	(65.3; 120.0)	(-34.5; 117.7)	(45.6; 82.9)	(78.4; 72.5)	(45.7; 71.1)	(16.7; 59.2)	(19.9; 58.0)	(12.8; 58.1)
B	(4.1; 52.5)	(-0.7; 52.7)	(0.5; 30.6)	(48.3; 29.4)	(-1.0; 17.9)	(15.3; 18.1)	(-0.7; 16.2)	(5.3; 16.7)
	(-1.5; 103.9)	(7.4; 104.1)	(-33.7; 50.4)	(123.3; 52.8)	(-1.4; 33.3)	(39.2; 34.8)	(3.4; 32.1)	(1.3; 32.8)
	(35.5; 59.0)	(-39.7; 59.6)	(36.8; 39.8)	(24.2; 36.9)	(27.7; 33.3)	(-20.0; 31.0)	(15.5; 27.3)	(-17.9; 30.5)
	(77.7; 120.6)	(-83.4; 122.0)	(58.1; 83.8)	(29.5; 79.3)	(58.2; 72.2)	(-32.2; 67.4)	(32.4; 59.3)	(-36.1; 66.4)
C	(24.0; 53.9)	(-22.2; 54.2)	(20.3; 33.0)	(26.7; 32.1)	(18.9; 21.7)	(-6.3; 22.1)	(19.2; 20.3)	(-16.2; 21.0)
	(45.4; 106.6)	(-45.8; 107.0)	(13.3; 55.7)	(70.2; 58.1)	(45.5; 41.0)	(-13.9; 42.4)	(50.3; 40.0)	(-51.9; 40.8)
	(-4.4; 63.2)	(10.0; 61.4)	(-3.0; 45.8)	(73.8; 39.8)	(-12.1; 40.2)	(29.7; 34.4)	(-24.3; 35.5)	(31.8; 33.9)
	(-7.8; 130.1)	(10.7; 126.0)	(-27.5; 97.1)	(123.5; 85.3)	(-27.4; 87.2)	(61.9; 74.3)	(-53.2; 76.9)	(58.0; 73.4)
D	(25.3; 57.0)	(-15.4; 57.1)	(21.6; 37.8)	(33.5; 36.7)	(20.2; 28.6)	(0.5; 28.4)	(20.4; 27.5)	(-9.4; 27.5)
	(39.4; 113.0)	(-23.3; 113.0)	(7.2; 67.1)	(92.6; 68.7)	(39.5; 55.5)	(8.5; 56.0)	(44.3; 54.8)	(-29.4; 54.8)
	(34.7; 59.6)	(-36.7; 58.7)	(36.0; 40.7)	(27.2; 35.4)	(27.0; 34.3)	(-17.0; 29.1)	(14.7; 28.6)	(-14.9; 28.6)
	(84.5; 119.7)	(-77.8; 117.4)	(64.8; 82.5)	(35.1; 72.0)	(64.9; 70.6)	(-26.6; 58.6)	(39.1; 57.4)	(-30.5; 57.5)
E	TB2, 500 N·m	TB2, -500 N·m	(-3.7; 58.2)	(48.9; 57.5)	(-5.1; 52.7)	(15.9; 52.6)	(-4.9; 52.1)	(6.0; 52.2)
	TB2, 1000 N·m	TB2, -1000 N·m	(-32.1; 110.5)	(115.9; 111.5)	(0.2; 103.9)	(31.8; 104.1)	(4.9; 103.5)	(-6.1; 103.5)
	TT1, 500 N·m	TT1, -500 N·m	(1.3; 61.9)	(63.9; 57.6)	(-7.7; 57.9)	(19.7; 54.0)	(-19.9; 54.7)	(21.8; 53.7)
	TT1, 1000 N·m	TT1, -1000 N·m	(-19.6; 125.1)	(112.9; 116.2)	(-19.6; 117.6)	(51.2; 108.3)	(-45.4; 110.2)	(47.3; 107.7)
F *	(3.7; 58.2)	(-48.9; 57.5)	TB2, 500 N·m	TB2, -500 N·m	(-1.4; 30.9)	(-33.0; 29.3)	(-1.2; 30.0)	(-43.0; 28.5)
	(32.1; 110.5)	(-115.9; 111.5)	TB2, 1000 N·m	TB2, -1000 N·m	(32.3; 50.2)	(-84.1; 52.8)	(4.8; 49.4)	(-122.1; 51.5)
	(-1.3; 61.9)	(-63.9; 57.6)	TT1, 500 N·m	TT1, -500 N·m	(-9.1; 38.2)	(-44.1; 27.0)	(-21.3; 33.2)	(-42.0; 26.4)
	(19.6; 125.1)	(-112.9; 116.2)	TT1, 1000 N·m	TT1, -1000 N·m	(0.1; 79.5)	(-61.6; 56.0)	(-25.8; 68.0)	(-65.6; 54.9)
G	(5.1; 52.7)	(-15.9; 52.6)	(1.4; 30.9)	(33.0; 29.3)	TB2, 500 N·m	TB2, -500 N·m	(0.3; 16.8)	(-9.9; 16.4)
	(-0.2; 103.9)	(-31.8; 104.1)	(-32.3; 50.2)	(84.1; 52.8)	TB2, 1000 N·m	TB2, -1000 N·m	(4.8; 31.9)	(-38.0; 32.8)
	(7.7; 57.9)	(-19.7; 54.0)	(9.1; 38.2)	(44.1; 27.0)	TT1, 500 N·m	TT1, -500 N·m	(-12.2; 24.9)	(2.1; 17.1)
	(19.6; 117.6)	(-51.2; 108.3)	(-0.1; 79.5)	(61.6; 56.0)	TT1, 1000 N·m	TT1, -1000 N·m	(-25.8; 53.0)	(-3.9; 35.4)
H	(4.9; 52.1)	(-6.0; 52.2)	(1.2; 30.0)	(43.0; 28.5)	(-0.3; 16.8)	(9.9; 16.4)	TB2, 500 N·m	TB2, -500 N·m
	(-4.9; 103.5)	(6.1; 103.5)	(-37.1; 49.4)	(122.1; 51.5)	(-4.8; 31.9)	(38.0; 32.8)	TB2, 1000 N·m	TB2, -1000 N·m
	(19.9; 54.7)	(-21.8; 53.7)	(21.3; 33.2)	(42.0; 26.4)	(12.2; 24.9)	(-2.1; 17.1)	TT1, 500 N·m	TT1, -500 N·m
	(45.4; 110.2)	(-47.3; 107.7)	(25.7; 68.0)	(65.6; 54.9)	(25.8; 53.0)	(3.9; 35.4)	TT1, 1000 N·m	TT1, -1000 N·m